compuscript

Acta Materia Medica

Review Article

Mass spectrometry imaging advances and application in pharmaceutical research

Xiaowei Song[a,*], **Chao Li**[b], **Yifan Meng**[c]

[a]Department of Chemistry, Fudan University, Shanghai, 200438, China
[b]Division of Nephrology, Department of Medicine, Stanford University School of Medicine, Palo Alto, 94304, CA, USA
[c]Department of Chemistry, Xiamen University, Xiamen, 361005, China

***Correspondence:** songxw@fudan.edu.cn (X. Song)

Received: 4 November 2022; Revised: 10 December 2022; Accepted: 13 December 2022

Published online: 23 December 2022

DOI 10.15212/AMM-2022-0046

ABSTRACT

Mass spectrometry imaging (MSI) has been shown to be a valuable tool through nearly every stage of the preclinical drug research and development (R&D) pipeline, and even to the early phase of clinical pharmaceutical evaluation. MSI can specifically resolve distributions of a parent drug and its metabolic products across dosed specimens without loss of spatial information, thus facilitating the direct observation of a drug's pharmacokinetic processes, such as absorption, distribution, metabolism, and excretion. MSI can simultaneously visualize hundreds of phenotype molecules, including proteins, glycans, metabolites, and lipids, which have unique distribution patterns and biofunctions across different physiologic regions. This featured specificity in the chemical and physical spaces empowers MSI as an ideal analytical technique in exploring a drug's pharmacodynamic properties, including *in vitro*/*in vivo* efficacy, safety, potential toxicity, and possible molecular mechanism. The application of MSI in pharmaceutical research has also been expanded from the conventional dosed tissue analysis to the front end of the preclinical drug R&D pipeline, such as investigating the structure-activity relationship, high-throughput *in vitro* screening, and *ex vivo* studies on single cells, organoids, or tumor spheroids. This review summarizes MSI application in pharmaceutical research accompanied by its technical and methodologic advances serving this central demand.

Keywords: mass spectrometry imaging, drug metabolism and pharmacokinetics, toxicology, *in vitro* efficacy evaluation, pharmaceutical research and development

1. INTRODUCTION

Mass spectrometry imaging (MSI) is not only the subject of extensive studies in academics, but also of wide interest in the pharmaceutical industry [1, 2]. MSI can directly acquire the molecular profile and visualize the spatial distribution of each ionized compound across a sample, particularly biological tissues. As one of the most promising and developing techniques in exploring spatial multi-omics, MSI is able to locate the drug and metabolite distribution but also provides insight into the phenotype changes underlying disease progression and drug intervention. In this article basic MSI workflow and technical advances will be introduced. Thereafter, the application of MSI in pharmaceutical research and future directions will be further elaborated and prospectively discussed.

2. GENERAL WORKFLOW OF MSI

The general MSI workflow for a preclinical pharmaceutical study is shown in **Figure 1**. Using a whole-body section from a dosed rat as an example, the test rat will be euthanized at the setup time point after drug administration. The body will be immediately harvested, frozen, and fixed into embedding gel for the follow-up cryo-sectioning process. After sufficient dehydration, the cryo-sectioned whole-body sample will be mounted on a 2D moving stage and hit by an *in situ* ionization probe either in spot-by-spot scanning with a pulsed laser/ion beam or in line-by-line scanning with continuous electrospray/plasma. The exogenous drug along with endogenous components located in each impact region can be instantly desorbed, ionized, and transported into an MS system for MSI data acquisition.

©2022 The Authors. Creative Commons Attribution 4.0 International License

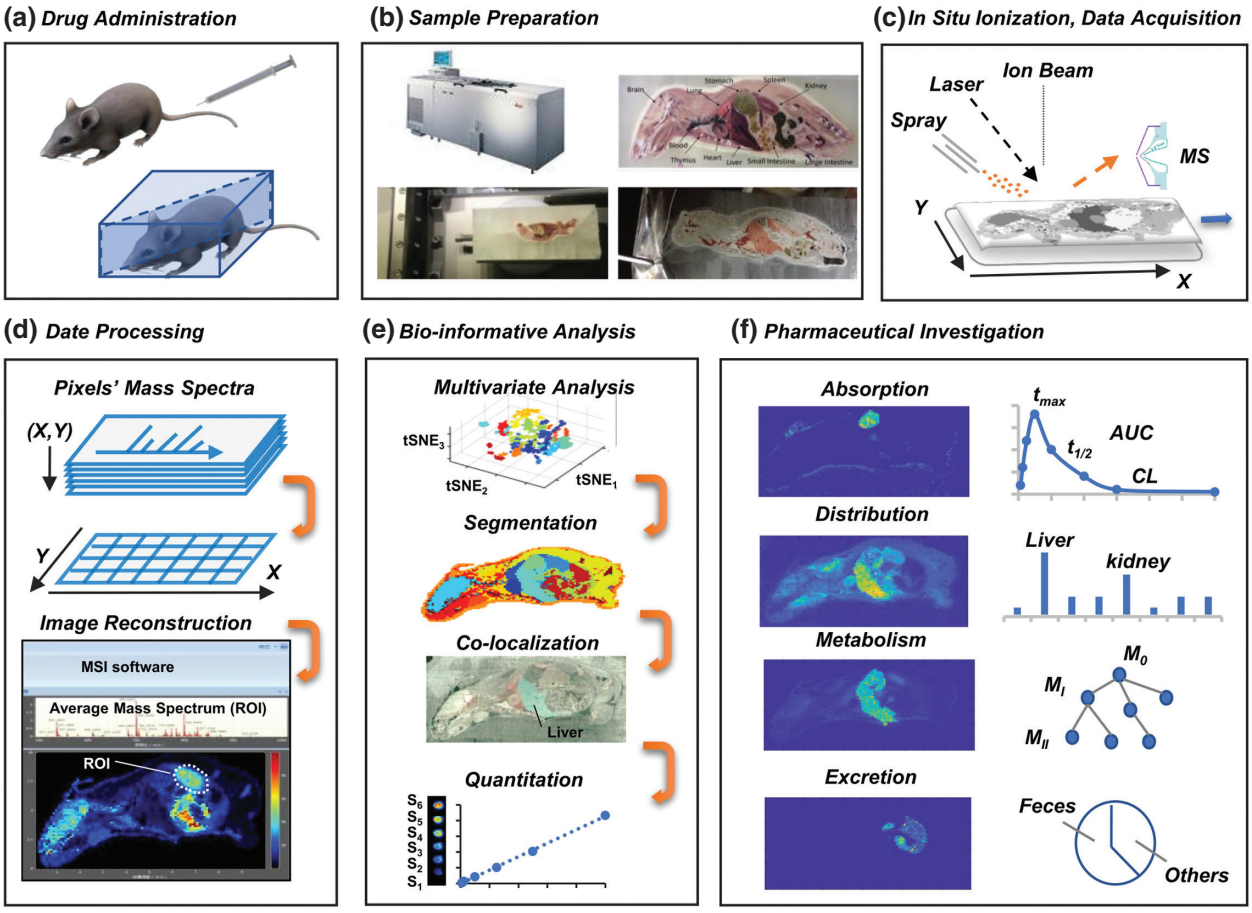

Figure 1 | Diagram illustration of the general MSI workflow in pharmaceutical research.
(a) The model mouse was euthanized, frozen, and fixed in the embedding medium after being dosed with the test drug; (b) A cryosection was prepared and transferred onto a loading slide and dehydrated before use; (c) The cryosection was mounted on a 2D moving stage and scanned by the *in situ* ionization probe that uses electrospray solvent, a laser beam, or ion beam; The local components were ionized and transported into a mass spectrometer for data acquisition; (d) Distribution of the drug and its metabolites across the whole-body section were imaged in available MSI software; (e) The precise localization of the drug was obtained by the guidance of optimal image or spatial segmentation by multivariate analysis based on region-specific molecular profile patterns; (f) The spatiotemporally-resolved ADME process was evaluated based on the relative abundance of the drug and its metabolites across different organs.

Thereafter, the MSI software will reconstruct any molecular image according to the ion intensity from each physical location, given a defined mass bin centered at the exact m/z of the target ion with a specified mass tolerance.

3. TECHNICAL ADVANTAGES OF MSI

The use of mass spectrometry for signal readout outperformed whole-body autoradiography (WBA) in drug distribution studies because MSI easily differentiates the parent drug and its metabolic product due to the *m/z* difference [3, 4]. In addition, MSI has thousands of available *m/z* channels for molecular profile recording compared to fluorescence or infrared-based spectroscopic imaging. Moreover, fluorescence or infrared-based spectroscopic imaging usually have very limited wavelength choices for multiplex display because of the bandwidth overlap. Liquid chromatography-mass spectrometry (LC-MS) continues to be the gold standard method to investigate the pharmacokinetic properties of a drug, including absorption, distribution, metabolism, and excretion (ADME); however, LC-MS is time- and labor-intensive with respect to sample pre-processing, including extraction, purification, and enrichment. This bulk measurement only reflects average levels of the drug and its metabolites in each organ or tissue region. More detailed spatial information associated with the efficacy or toxicity will be inevitably sacrificed because of the vigorous tissue disruption process. In contrast, MSI

©2022 The Authors. Creative Commons Attribution 4.0 International License

Acta Materia Medica

achieves direct desorption and ionization of analytes from the biological tissue sample surface. More precise drug localization information can be preserved at the sub-organ, tissue microcompartment, or cellular level depending on the physical size of the impact region by an ionization probe.

4. AVAILABLE CHOICES FOR *IN SITU* IONIZATION

The development of *in situ* ionization, as the core of MSI, is always the central task to drive the progress of MSI advances both in sensitivity and spatial resolution. Nevertheless, in most situations, sensitivity and spatial resolution are a pair of trade-off metrics when choosing a suitable *in situ* ionization method. Higher spatial resolution means less impact area and desorbed sample amount for feeding the follow-up detection. In turn, an increase in the impact area may help to raise the detection sensitivity, but at the cost of poor spatial resolution. Extensive efforts are still urgently needed to pursue an in-depth coverage of chemical species and precise observation of a drug's process within intricate physiologic structures or organelles at a few microns and even nanometer scale.

To date, various *in situ* ionization methods have been extensively developed; representative *in situ* ionization methods are shown in **Table 1**. According to the types of desorption and ionization source, major impact probes include laser (e.g., matrix-assisted laser desorption/ionization [MALDI]), ion beam (e.g., secondary ion mass spectrometer [SIMS]), plasma (e.g., dielectric barrier discharge ionization [DBDI]), and charged microdroplet spray (e.g., desorption electrospray ionization [DESI]), The former two typically work in a closed, vacuum environment. The desorbed and ionized species have less of a chance to collide with the air and introduce the external interfering components during the travel from the sample surface into the MS inlet. Intricate instrumentation design and relatively higher cost are needed for laser/ion beam focusing, transmission, and vacuum maintenance. Development of the DESI was an evolutionary breakthrough and opened a new era of ambient ionization [5]. Ambient ionization-based MSI liberates the sample analysis from the vacuum condition, avoids

Table 1 | *In situ* ionization methods for mass spectrometry imaging experiment in pharmacy.

Ionization	Matrix	Vacuum	Typical resolution	Chemical species	Ref.
MALDI (Matrix-assisted laser desorption ionization)	Y	Y	25-50 μm	Proteins, organic drugs	[134]
MALDI-II	Y	Y	<10 μm extreme: 200 nm	Proteins, small organic drugs	[11]
AP-MALDI (Atmospheric pressure-MALDI)	Y	N	10-30 μm extreme: 1.4 μm	Proteins, small organic drugs	[135]
LA-ICP (Laser ablation-inductively coupled plasma)	N	Y	5-200 μm	Metal-labels on antibody or organometallic drug; <200 Da	[136]
LAESI (Laser ablation electrospray ionization)	N	N	150-400 μm extreme: 5 μm	Small organic drugs	[137, 138]
IR-MALDESI (Infrared matrix-assisted laser desorption electrospray ionization)	Y	Y	45-200 μm	Proteins, small organic drugs	[139, 140]
DESI (desorption electrospray ionization)	N	N	100-200 μm	Small organic drugs	[5, 6, 141]
AFA-DESI (air flow-assisted DESI)	N	N	100-200 μm extreme: 50 μm	Small organic drugs	[21]
Nano-DESI	N	N	10-25 μm	Proteins, small organic drugs	[142]
LESA (Liquid extraction surface analysis)	N	N	>200 μm	Proteins, small organic drugs	[143, 144]
SIMS (secondary ionization mass spectrometry)	N	Y	50 nm	Metal-based organic drugs <500 Da	[145]
nanoSIMS	N	Y	<50 nm	Metal-based drugs	[146]

©2022 The Authors. Creative Commons Attribution 4.0 International License

the use of a matrix, and greatly lowers the technical barrier and analytical cost for an MSI experiment [6]. Versatile ambient ionization methods are under explosive development in the past decade [7].

Each ionization method has unique advantages and limitations in suitable chemical species, spatial resolution, matrix use, or ambient/vacuum operation. Selecting a suitable ionization source should systematically consider the physiochemical properties of the drug, the specific physical size of the sample, and the physiologic structure of interest. Generally, MALDI, DESI, and SIMS, as three major ionization sources in MSI, are top choices for imaging biotherapeutics, low molecular weight organic synthesis drugs, and metal-based drugs, respectively. DESI has a typical lateral resolution of 50-100 μm, whereas MALDI has a typical resolution of 20-50 μm. Therefore, DESI and MALDI can be used for conventional analyses of whole-body animals, organs, or tissues at the mm scale. Recent reports showed that DESI resolution had substantial improvement and robust performance by modifying the co-axial spraying capillary setup or introducing a ring-electrode for focusing highly-dispersed spraying [8, 9]. Introducing a well-designed optical pathway and a focusing system could also sharpen the impact laser point to a few microns or even a sub-micron scale, thus enabling laser-based MSI (e.g., MALDI and laser ablation-inductively coupled plasma-mass spectrometry [LA-ICP-MS]) collect the cellular-resolved images [10, 11]. SIMS has the highest spatial sub-micron resolution (approximately 300 nm) compared to the above-mentioned sources. This advantage makes SIM the first choice for observing cellular or sub-cellular biological process for *in vitro* drug research [12, 13]. Considering that this review emphasizes pharmaceutical applications, more details in ionization principles, instrumentation, and underlying mechanisms will not be exhaustively elaborated, which can be referenced to the corresponding literature according to the reader's special interests [14-16].

5. MSI SENSITIVITY

Sensitivity is another challenging issue facing MSI practical use in pharmaceutical analysis. For technical reasons, the MSI advantage in free-of-sample pretreatment is built on the *in situ* ionization of drug molecules from the biological sample. Thus, the complex composition of a biomatrix will inevitably compete with the drug molecule and suppress ionization efficiency, which is known as the matrix effect [17]. From a pharmacology perspective, an effective drug candidate with a higher potency means a lower dose to reach the minimum therapeutic level, which may also cause false-negative detection by MSI. From the pharmacokinetic perspective, first-pass elimination lowers the effective concentration of a drug administered through the non-intravenous route, particularly the oral pathway. Given these reasons, drug distribution results acquired using the MSI technique need to be carefully validated via conventional liquid chromatography-tandem mass spectrometry (LC-MS/MS)-based drug measurement as the complementary reference to avoid false-negative results, especially when the single dose is less than the mg/kg level.

Enormous effort has been expended in instrumentation and the MSI methodology to overcome limited sensitivity. Photon-based post-ionization (UVPD) or secondary ionization (MALDI-2) techniques were developed to fully ionize non-polar, neutral molecules [11, 18, 19]. For ambient ionization, the DESI prototype configuration has undergone innovative improvement (air-flow-assisted DESI [AFA-DESI]). A local vacuum chamber is coupled with the MS inlet and connected with the transport tube from the sampling end in this set-up. The gas pressure gradient focuses and directs random airflow to pick up additional molecules splashed from the tissue into the MS system for detection [20, 21].

New functional matrices have been developed for MALDI to avoid severe interference at the lower mass range and facilitate laser desorption ionization of chemical species [22]. Various nanomaterials are fabricated as the sample loading/imprinting substrate or energy absorption/transfer medium to enhance the target detection [23]. On-tissue chemical derivatization gains increasing attention for those species which have low abundance, less stability, weak polarity, or poor ionization efficiency, such as steroids, thiols aldehydes, and alkenes [24, 25]. Derivatization reagent can be introduced through matrix spraying, vaporization, or photon irradiation in a closed chamber [26-28]. Solvent immersion can be a cleanup process to remove those unwanted species and enhance the target analyte's sensitivity [29, 30]. Alternatively, the hydrogel has also been proven to be a biocompatible and tissue-friendly medium to conduct *in situ* desalting, digestion, cleavage, and derivatization with no severe tissue disruption [31].

6. MSI DATA ACQUISITION

The peak capacity of an MSI method relies heavily on the performance of a mass analyzer. Currently, to fulfill the task of collecting increasing data volume in spatial omics research, a high-resolution mass spectrometer (HR-MS) has become the mainstream device with an orbitrap, quadrupole time-of-flight (QTOF), and Fourier-transform ion cyclotron resonance (FTICR) as three representative types. A full scan is the default mode to acquire as much abundant phenotype information as possible to present untargeted metabolic or proteomic profiles. HR-MS also provides the exact *m/z* value for a more convincing annotation of the ion identity. A more authentic spatial information specific to a relatively "pure" ion can be achieved by filtering the interfering ions that *m/z* are extremely close to the target [21].

The triple quadrupole and linear ion trap are low-resolution tandem mass analyzers that are mainly used for quantitative and qualitative analyses of drug

©2022 The Authors. Creative Commons Attribution 4.0 International License

concentration and metabolism in an LC-MS/MS system. The triple quadrupole and linear ion trap can also be used to conduct MSI studies in special situations. Selected reaction monitoring (SRM) has become the alternative choice for targeting drugs and the active/toxic metabolic products if the drug exists in a low concentration and is too weak to be detected by the full scan or the target ion has severe isobaric ion interference [32, 33]. An $MS^{(n)}$ scan performed by a linear ion trap is mainly used for identifying those region-specific marker ions.

Additionally, ion mobility mass spectrometry (IMS) has gained popularity among MSI users in recent years because of unique technical features in isomer separation [34]. These isomers sharing the identical *m/z* can be differentiated to achieve a separate spatial distribution. Interfering components will also be filtered out of the expected traveling time window to increase the target ion intensity. Coupling in the front end of an MS system creates a new dimension for molecular profiling and broadens the scope of observable species by MSI [35].

7. MSI DATA ANALYSIS

An MSI experiment generates gigabytes of big data that contains thousands of ion information for follow-up data processing. The collected MSI data relies heavily on the software or a self-written code to be translated into spatially-resolved molecular information. There is more than one choice of available MSI software developed for reader reference and practice (**Table 2**). Basic MSI data pre-processing includes mass peak picking, alignment, and normalization. The basic function of MSI software includes ion image construction, region of interest (ROI) delineation, and average mass spectrum generation. Commercial and open-access software is a user-friendly choice to researcher convenience [36].

Apart from the graphic user interface (GUI)-based software, self-programing is another choice for developers who are engaged in the new MSI function and computation method [37]. The new MSI data computation method can be promptly translated into real practice when implemented in environments, such as RStudio, Python, MATLAB, and Delphi. Multivariate analytic methods, machine learning, and deep learning models are introduced into the MSI data processing tasks, such as automatic spatial segmentation [38, 39], discriminative ion picking and latent feature extraction [40-42], region-specific matrix effect normalization [43], 3D image construction [44, 45], high-quality image recovery by over- or sparse-sampling [46, 47], co-localization (co-registration) among multi-modal images [48, 49], and spatial multi-omics imaging data integration [50, 51].

8. QUANTITATIVE MSI

MSI presents the relative abundance of a drug according to the normalized ion intensity across the tissue section. Unfortunately, tissue structural and compositional heterogeneity causes severe variance in the ionization efficiency of the drug. This region-specific matrix effect may distort the linear response of a drug ion intensity with the local concentration [43, 52, 53], thus biasing the comparison of drug distribution across different regions. The quantitative MSI method (QMSI) has been well-developed to overcome this issue and obtain an accurate spatially-resolved content difference of the drug. The tissue-specific ion suppression can be well-compensated by deuterated internal standards, chemometric calibration [54], or external evaluation of the tissue signal extinction coefficient [55]. A dilution series of drug and internal standards can be incorporated into a blank tissue to serve as the simulative dose one by several strategies, including the on dry tissue method (the most frequently used) [56], under wet tissue method [57], in-tissue homogenate [58], and in biomimetic 3D tissue [59]. Another alternative strategy is to introduce laser-capture microdissection (LCM) to harvest numerous tiny tissue regions of interest for follow-up LC-MS/MS measurement [60, 61]. The drug content is reported as the molar amount per area (i.e., pmol/mm^2) or the weight percentage (i.e., μg/g). Although each strategy cannot guarantee completely identical ionization behavior with a native drug, the LC-MS/MS cross-validation result reveals a system error that is usually within an acceptable range (±15%) for drug quantitation in the drug metabolism and pharmacokinetics (DMPK) study.

9. SPATIAL CO-LOCALIZATION

Precise localization of drug molecules in a physiologic structure is a prerequisite to learn about the distribution in targeted and non-targeted regions. The drug ion image cannot provide an accurate map of intact tissue outlines and structural microregions. A guiding map of the region can be accessed from three strategies: (1) region-specific endogenous metabolite as the marker, such as heme, which can delineate the blood vessels [62, 63]; (2) MSI data-driven spatial segmentation, which can be performed with the aid of a machine learning or deep learning method to split all biological image pixels into several groups of micro-regions according to the molecular profile patterns; frequently used methods include principal component analysis (PCA), partial least square discriminant analysis (PLS-DA), t-stochastic neighbor embedding (t-SNE), KMeans clustering, uniform manifold approximation and projection (UMAP), and convolutional neural network [64]; (3) a complementary image that can be acquired from an optical microscopy image of a biological sample hematoxylin and eosin stain (the most frequently used) [65, 66], bright-field polarimetry [67, 68], immunohistochemistry (IHC) [69], molecular imaging, such as fluorescence microscopy [70], and Fourier transfer infrared microscopy [71], nuclear medicinal imaging technique, such as magnetic resonance imaging (MRI) [72], and positron emission tomography/computer tomography (PET/CT) [73].

©2022 The Authors. Creative Commons Attribution 4.0 International License

Table 2 | Available software, package, or platform for mass spectrometry imaging data analysis.

Software	Availability	Ionization dependence	Data format	Featured functions apart from basic visualization**	Ref.
M^{2}aia	Open-source	NS*	imzML	Prep; MIO; Seg; manual alignment feature extraction; dimension reduction	[147]
MSiReader	Open source	NS*	imzML	QMSI; MIO; ROI, Mass Measurement Accuracy Heatmap and Histograms; Multiple sample loading	[148, 149]
BioMap	Open-source	MALDI	Analyze 7.5, TIF, DICOM, PNP	MIO; 3D; ROI	[150]
omniSpect	Open-source	DESI, MALDI	Analyze 7.5, mzXML, cdf	MVA	[151]
Mirion	Open-source	NS*	imzML	Automatic processing; Automatic image generation; MIO	[152]
msIQuant	Open-source	MALDI		QMSI; BDP; MIO	[153]
Cardinal	Open-source	DESI, MALDI	imzML	Seg; Stata	[154]
Pew^2	Open source	LA-ICP	Agilent Batch; PerkinElmer XL; Thermo Qtegra	MIO; ROI; QMSI	[155]
DataCube Explorer	Open source	NS*	imzML	Prep; 3D; ROI	[156]
OpenMSI	Open source	NS*	xml	Web-based API for remote access and processing, URL-based data analysis sharing; BDP	[129]
MITICS	Open-source	MALDI	xml	MSI; AVG; ROI	[157]
rMSIannotation	Open source	NS*	imzML	Peak annotation; isotopic peak removal; adduct ion recognition	[119]
SpectralAnalysis	Open source	DESI, MALDI	imzML	Prep; MVA	[158]
LipostarMSI	Open source	NS*	imzML	Prep; ROI; Stata; MVA; MIO; automated identification	[118]
MassExplorer	Open source	DESI	csv	Prep; Stata; ML; FS	[159]
Massimager	Commercial	NS*	cdf, mzXML	Prep; ROI; AVG; MIO; FS; MVA; I/E	[160, 161]
FlexImaging	Commercial	MALDI	imzML	Prep; ROI; AVG; MVA	[162]
SCiLS Lab	Commercial	MALDI	imzML	Prep; ROI; AVG, Seg; MIO; 3D; I/E; Extensive API	[163]
TissueView	Commercial	MALDI	imzML	AVG; ROI; MIO	—
HDImaging	Commercial	DESI, MALDI	imzML	MIO; Streamline processing	—

*NS: not specified.
**3D:3D imaging; QMSI: quantitative MSI; AVG: average mass spectrum generation; BDP: big data processing; ROI: region of interest selection; Pre: spectral pre-processing steps including peak picking, baseline smoothing, data transform; MIO: Multimodular images overlay; Seg: spatial segmentation; Stat: statistical description and feature extraction; ML: machine learning; I/E: import and export; FS: feature selection; API: application programming interface.

10. DRUG METABOLISM AND PHARMACOKINETICS

In preclinical drug research and development (R&D), the assessment of the drug candidate's distribution is a central concern for a better understanding of its efficacy and possible toxicity at the early stage of *in vivo* investigation. DMPK testing became the first *in vivo* study to decide whether a drug candidate deserves further investigation or suspension. Although drug concentrations in plasma/serum are indicative of DMPK properties, it has

©2022 The Authors. Creative Commons Attribution 4.0 International License

Table 3 | Representative study cases of mass spectrometry imaging in preclinical and clinical pharmaceutical research.

Application	Sample	Drugs	Metabolic product	Quantitation	Ionization	Mass analyzer	Complementary methods	Ref.
First-pass effect	CD57 mice and SD rat whole-body	Clozapine, terfenadine, fexofenadine, ketoconozole	Y	N	MALDI	QqTOF	LC-MS/MS	[164]
Blood-brain barrier	Mouse brain with PVL311 xenograft tumor	Erlotinib, and two drug candidates (BKM120, RAF265)	N	N	MALDI	TOF	Fluorescence H&E staining	[63]
Blood-tumor barrier	Mouse brain with metastases of the lung cancer	Epertinib, lapatinib	Y	Y	MALDI	LTQ	Bioluminescent image H&E Staining IHC, LC-MS/MS	[165]
Dermal permeation	Human/rat skin	Saxitoxin, neosaxitoxin, batrachotoxin, aconitine	N	N	DESI	Orbitrap	H&E Staining	[79]
Targeting	Xenografted tumor	Paclitaxel derivatives	Y	Y	AFA-DESI	Orbitrap	H&E Staining	[77]
Targeting	Patient-Derived Xenografts (PDX)	Paclitaxel	N	Y	MALDI	TOF	H&E Staining LC-MS/MS	[166]
Targeting	Rabbit lung	Moxifloxacin	N	Y	MALDI	QTRAP	LC-MS/MS H&E Staining	[76]
Sustained release	Implanted hydrogel	Celecoxib nanoparticles	N	N	DESI	orbitrap	Immunofluorescence	[167]
Penetration	Necrotic Granulomas in lung tissue	Clofazimine, moxifloxacin, bedaquiline, pyrazinamide, rifampicin	N	N	AP-MALDI	orbitrap	H&E Staining	[168]
Penetration	Triple negative breast cancer xenograft tumor on rat	Veliparib and carboplatin	N	Y	MALDI, LA-ICP	TOF Quadrupole	MRI, LC-MS, H&E Staining	[169]
Absorption	Rat intestine	Polyphenol (theaflavin-3'-O-gallate; epicatechin-3-O-gallate)	Y	N	MALDI	TOF	LC-MS	[170]
CNS distribution	Monkey, Rabbit brain	Fosdevirine (GSK2248761)	Y	N	MALDI	TOF	LC-MS/MS	[95]
Drug distribution	Neoplastic and normal tissues	Pioglitazone	N	Y	AP-MALDI	orbitrap	HPLC-UV	[171]
Drug distribution	Colon cancer murine model; transversal whole-body tissue	Irinotecan and its active metabolite SN-38	Y	N	MALDI	TOF, FT-ICR	Immunohistochemical staining	[172]
Drug distribution	Cervical tissue model	Emtricitabine	N	Y	IR-MALDESI	orbitrap	LC-MS/MS	[173]
Drug distribution	Rat liver, and kidney	Atorvastatin	Y	N	MALDI	orbitrap	LC-MS	[174]
Drug distribution	Neonate mice whole-body	Clozapine, and three unknown compounds	N	N	DESI	orbitrap	H&E staining LC-MS	[175]
Drug distribution	Rat whole-body Mouse bearing neuroglioma	Deoxytylophorinidine (CAT)	Y	Y	AFA-DESI	QTRAP	H&E staining LC-MS/MS	[176]
Drug distribution	Human tumor	Cisplatin, oxaliplatin	N	N	LA-ICP MALDI	Quadrupole TOF/TOF	Optical microscope	[80]

© 2022 The Authors. Creative Commons Attribution 4.0 International License
Acta Materia Medica

Table 3 | Continued

Application	Sample	Drugs	Metabolic product	Quantitation	Ionization	Mass analyzer	Complementary methods	Ref.
Pharmacokinetics	Mouse spleen	Cucumarioside A2-2	N	Y	MALDI	TOF	Radiospectroscopy	[177]
Correlation of drug distribution with vascularization	Xenografted tumor	Afatinib, erlotinib, sorafenib	N	N	MALDI	TOF	Immunohistochemical staining	[74]
Cassette-Dosing High throughput PK	Rat kidney	Haloperidol, bufuralol, midazolam, clozapine, terfenadine, erlotinib, olanzapine, moxifloxacin	N	N	MALDI, DESI, LESA	QqTOF, QTRAP, FTICR	Optical microscope	[62]
Drug-drug interaction	Mice brain	Propranolol, loperamide	N	Y	DESI MALDI	Orbitrap TOF/TOF	H&E staining	[178]
SAR	Rat brain	*Uncaria* indole alkaloids	N	Y	DESI	QTOF	H&E staining	[102]
Metabolism	Whole-body mouse Kidney, intestine	Cyclosporine	Y	Y	DESI / MALDI	Orbitrap		[179]
Metabolism and hepatotoxicity	C57BL/6J mice liver	Acetaminophen	Y	N	DESI	QTOF	LC-MS/MS	[180]
PK/PD	Squamous Cell Carcinoma of the Head and Neck from patients	Xevinapant	N	N	MALDI	FT-ICR	LC-MS/MS H&E Staining	[81]
Safety and Toxicology	Zebrafish	Diazepam 2-methylamino-5-chlorobenzophenone	Y	N	DESI	TOF	H&E staining	[98]
Safety and Toxicology	Rat kidney	Bisphenol S	N	N	MALDI	TOF	LC-MS/MS	[94]
Safety and Toxicology	Wistar Hannover Galas rat kidney	Two tested compounds and their common metabolite bisulphonamide	Y	N	MALDI	QTOF	NMR LC-MS	[181]
Mechanism	Rat whole-body	NHBA	N	N	AFA-DESI	TOF; QqQ	LC-MS H&E staining	[83]
Mechanism	Rat brain	Scopolamine	N	N	AFA-DESI	Orbitrap	Nissl Staining	[84]
Cellular uptake	*In vitro* cultured HeLa cells	Carboplatin	N	N	LA-ICP	Quadrupole	Microscopy	[182]
Pharmaco-metabolomics	Rat brain	Scopolamine	N	N	AFA-DESI	Orbitrap	H&E staining	[84]
Pharmaco-metabolomics	Mouse lung, liver, kidney	Pirfenidone	Y	Y	MALDI	FTICR	—	[183]
In vitro evaluation	HCT 116 colon carcinoma multicellular spheroids	Irinotecan	N	Y	MALDI	FTICR	Nano-LC-MS	[130]
In vitro high-throughput screening	Live A549 lung cancer cells	Fatty acid synthase inhibitor GSK2194069	N	N	MALDI	TOF	Microscopy	[90]

© 2022 The Authors. Creative Commons Attribution 4.0 International License

Acta Materia Medica

been argued whether the plasma/serum concentrations alone can accurately reflect the localized drug concentration in tissue. Drug enrichment located in the target region may indicate the potential efficacy, whereas the unexpected accumulation in non-target tissue probably causes adverse effects or even toxicity. For conventional drug distribution measurement by LC-MS, bloodletting is a necessary step to diminish the influence of vascularization and the amount of blood infused. The unique advantage of MSI in spatially-resolving ability cannot only differentiate the drug and metabolites, but also the blood vessel and non-vessel regions, making MSI well-suited for the demands of DMPK studies, although MSI still depends on how well an MSI system can achieve spatial resolution. Currently, an MSI marker, such as heme (*m/z* 616), has been introduced to localize the blood vessel distribution or differentiate the blood vessel distribution from non-blood vessel regions within an organ [62]. Other imaging methods, such as immunohistochemical vessel staining, can also help to co-locate blood vessels and rule out their influence on blood vessel distribution [74].

Currently, MSI has been extensively applied to visualize the spatial distribution of a drug in animal models (**Table 3**). The distribution of a drug and its metabolites within intricate sub-organ structures or micro-compartments can be well-discerned. The MSI-observable object has a huge expansion that varies from mm to sub-microns in physical size, including *in vivo* samples, such as whole-bodies of rats or zebrafish, organs, tumors, tissues, and *ex vivo* samples, such as organoids and cultured cells (**Figure 2**). The Dome and Marko-Varga groups collaboratively characterized the distribution and metabolism of sunitinib in solid tumors, as well as kidney and liver by MALDI-MSI. Drug content was quantified, and the three metabolites were found to have close distribution patterns with the administrated parent drug (**Figure 3a-b**). Tumor growth and intra-tumor VEGF receptor-2 expression were significantly inhibited by sunitinib-treatment. There were intra-tumor areas where the signal intensity of sunitinib correlated with expression of VEGF receptor-2 [75]. Prideaux *et al.* used MALDI-MSI to investigate the targeting efficiency of the anti-tuberculosis (TB) drug, moxifloxacin, in TB-infected rabbit lungs. The drug was shown to accumulate granulomatous lesions at levels higher than the surrounding lung tissue from 1.5 h post-administration, which was quantitatively validated by LC-MS/MS (**Figure 3c**) [76].

The Zeper and He groups presented the use of air flow-assisted desorption electrospray ionization (AFA-DESI) in accurately quantifying the distribution of paclitaxel (PTX) and its prodrug (PTX-R) in whole-body sections of xenografted mice based on a previously developed virtual calibration quantitative MSI method (VC-QMSI) [43, 77]. Based on the machine learning-based spatial segmentation and signal calibration, the drug distribution in each organ and tumor micro-region was accurately discerned and quantified. AFA-DESI-MSI indicated that PTX is widely distributed in multiple organs throughout the dosed body in the PTX group, both in the form of through direct injection and liposome. In contrast, the PTX prodrug was enriched in the tumor tissue and catabolized to release more active PTX for anti-tumor action, particularly in the poorly differentiated intratumor and necrotic areas (**Figure 4a**). The relative targeting efficiency of PTX-R was

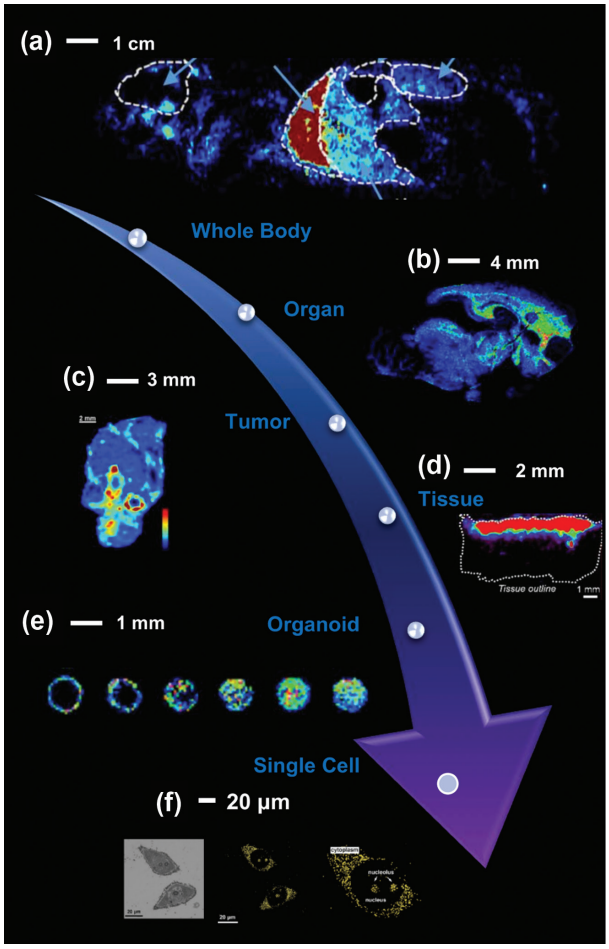

Figure 2 | Span in the physical size for biological samples tested by MSI in pharmaceutical research.
(a) The AFA-DESI-MS image of a drug candidate, LXY6006, across a whole-body mouse section [31]; copyright 2017 *American Chemical Society*. (b) MALDI-MS image of Fosdevirine cysteine conjugate distribution across the rabbit brain sagittal section [95]; copyright 2020 *American Chemical Society*. (c) AFA-DESI MS image of a paclitaxel derivative prodrug heterogenous enrichment in a xenograft tumor section [77]; (d) Penetration of lidocaine across the human skin visualized by DESI-MSI [79]; copyright 2014 *American Chemical Society*. (e) Time-dependent penetration of irinotecan in tumor spheroids analyzed by MALDI-IMS [130]; copyright 2013 *American Chemical Society*. (f) Image of single cells cultured with acriflavine detected by micro-lensed fiber laser desorption mass spectrometry imaging [131].

©2022 The Authors. Creative Commons Attribution 4.0 International License

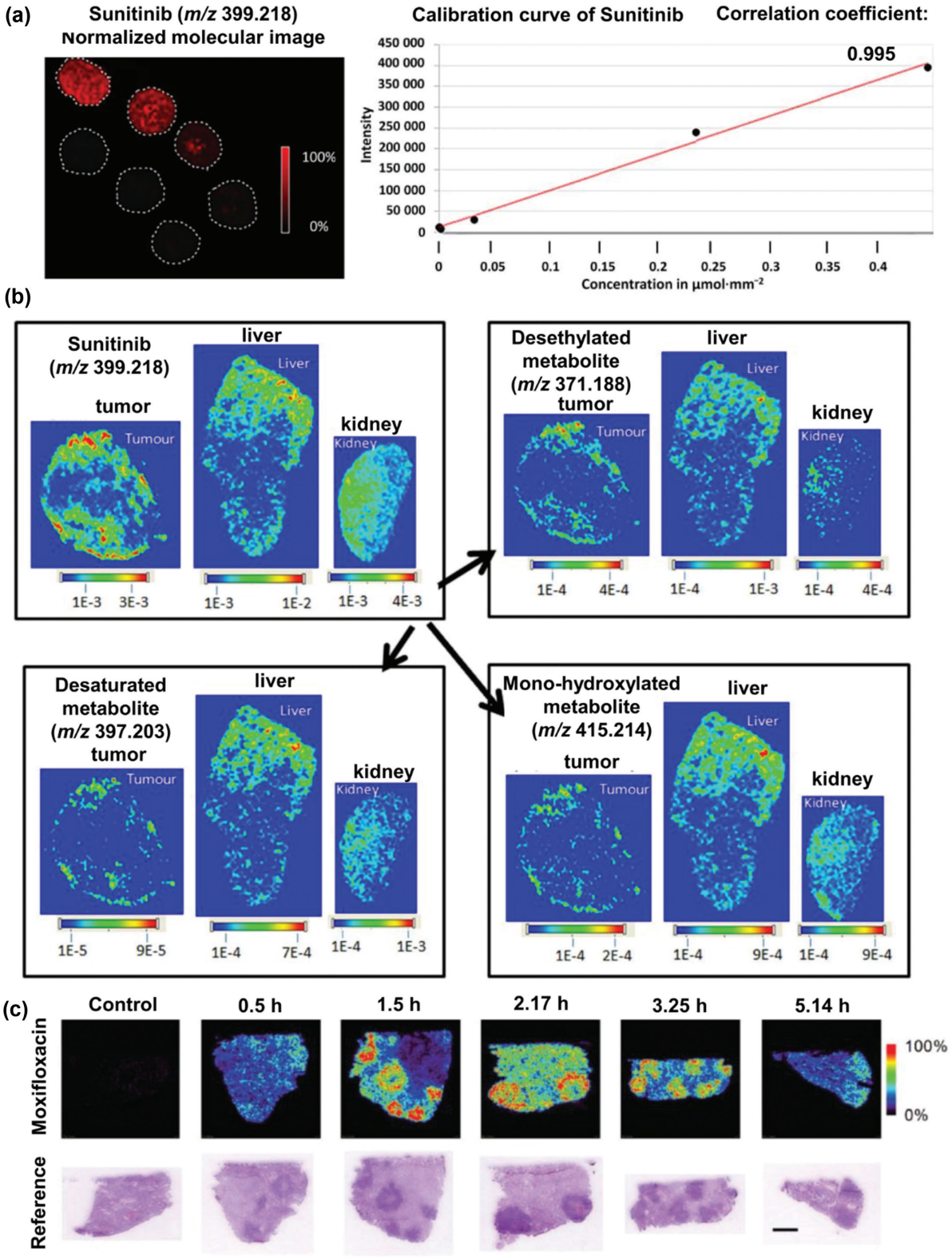

Figure 3 | Typical cases of MSI in the preclinical DMPK study.
(a) On-tissue strategy to construct simulated tissues for quantitation of sunitinib; (b) Sunitinib and three metabolic product distributions across the tumor, liver, and kidney [132]; (c) Spatiotemporal distributions of moxifloxacin within the rabbit lungs at different times after dosing [76]. copyright 2011 *American Chemical Society*.

©2022 The Authors. Creative Commons Attribution 4.0 International License

Acta Materia Medica

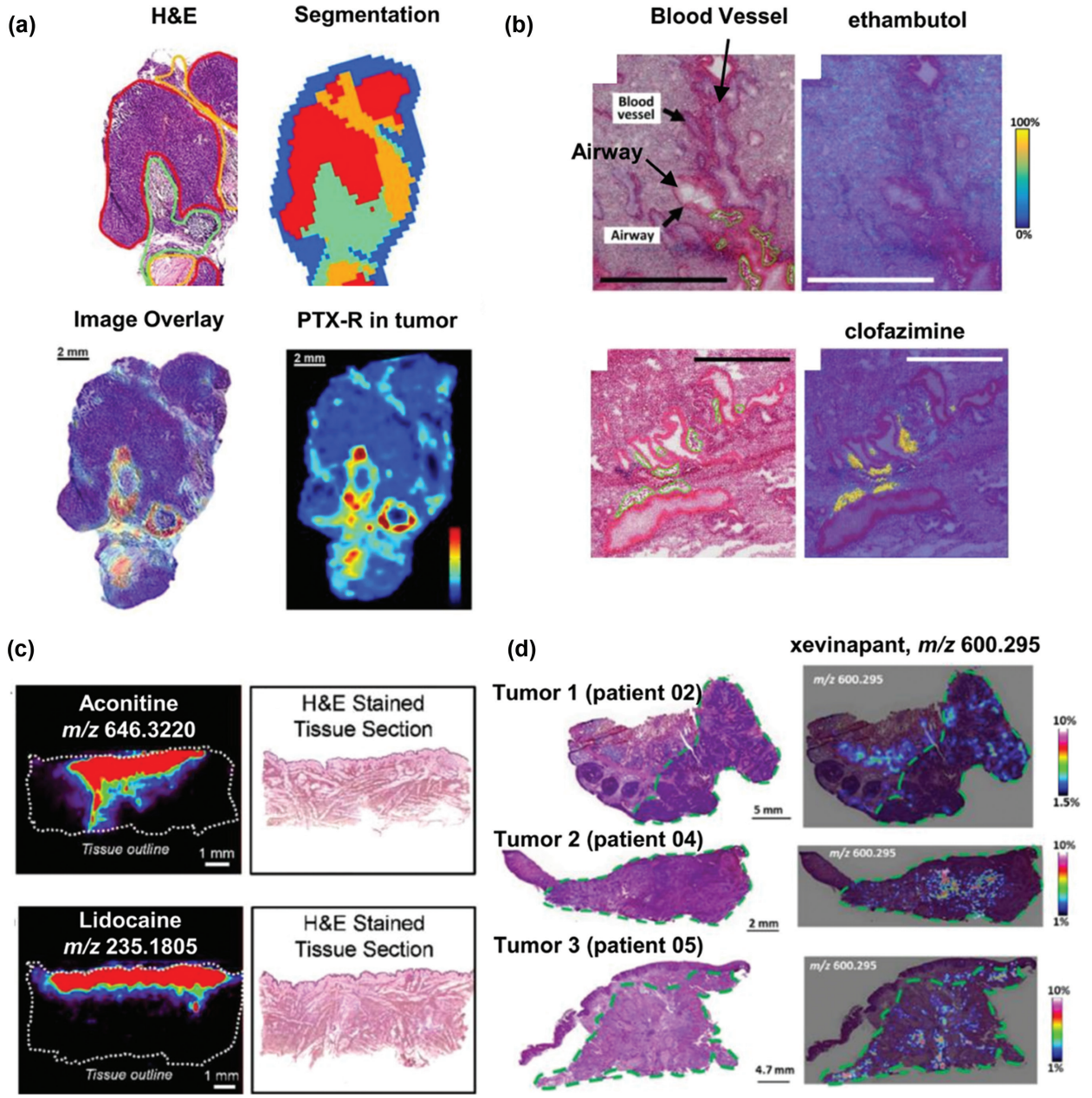

Figure 4 | Representative MSI cases in the preclinical and clinical pharmaceutical research for mapping drug penetration and enrichment in the target tissue.

(a) Images of H&E staining, data-driven spatial segmentation, and paclitaxel derivative prodrug within heterogenous xenograft tumor section and the overlay image [77]; (b) Overlay of the H&E stain with the ion images of ethambutol and clofazimine in the mouse lung lobe measured at 10-μm pixel size. H&E stain of the measurement field of view showing blood vessels and bronchioles. Adipocyte clusters are highlighted in green; Copyright 2020 *American Society for Mass Spectrometry*. Adapted with permission from reference [78]. (c) Penetration of aconitine and lidocaine across the human skin visualized by DESI-MSI [79]; copyright 2014 *American Chemical Society*. (d) Histologic images of tumor sections harvested from patients, and xevinapant distribution images overlayed with the H&E staining. Cancerous regions were delineated in green dash line. Copyright 2022 *American Chemical Society*. Adapted with permission from reference [81].

increased approximately 50-fold compared to the plain PTX injection [41]. The Römpp group developed a new MALDI-MSI method with excellent performance in mass (240k @ *m/z* 200 full width at half maximum [FWHM]) and spatial resolution (10 μm pixel size). Thereafter, four first-line anti-tuberculosis drugs (pyrazinamide, rifampicin, ethambutol, and isoniazid) and two second-line drugs (moxifloxacin and clofazimine) in murine

©2022 The Authors. Creative Commons Attribution 4.0 International License

lungs were successfully visualized in the expected action site of necrotizing granulomas. For the first time, clofazimine was imaged and revealed to be accumulated in lipid deposits around airways (**Figure 4b**) [78].

Apart from preclinical pharmaceutical studies, MSI has also been successfully translated into clinical drug trials and therapeutic drug monitoring for a better prognostic evaluation. Eberlin *et al*. used DESI-MSI to visualize the transverse distribution of several sodium modulators on the harvested human skin. The transdermal permeation process can be spatially resolved from the drug amount across the epidermis, dermis, and hypodermis (**Figure 4c**). Then, the skin structure-specific lipid compositions were characterized and further used to evaluate the compound protection and healing effects on the skin impairment after long-term ultraviolet exposure [79]. The Lobinski group combined LA-ICP-MSI and MALDI-MSI to evaluate the penetration of cisplatin and oxaliplatin in tumors resected from patients with colorectal or ovarian peritoneal carcinomatosis. The behavioral differences between oxaliplatin and cisplatin were confirmed by LA-ICP MSI. Oxaliplatin was enriched at the tumor periphery, whereas cisplatin penetrated deeper into the tumor core region [80]. Menetrey *et al.* used MALDI-QMSI to quantitatively evaluate the penetration and concentration of an apoptosis protein antagonist, xevinapant, in tumors resected from squamous cell carcinoma of head and neck (SCCHN) patients in a preoperative window-of-opportunity (WoO). The overall tumor-to-plasma ratio of 25 was determined, indicating a tumor penetration for xevinapant in the treatment of SCCHN patients (**Figure 4d**) [81].

11. *IN VIVO* DRUG EFFICACY AND MOLECULAR MECHANISM

Elucidation of the drug candidate action of mechanism is fundamental to evaluate drug efficacy. MSI can simultaneously acquire different types of endogenous metabolites apart from drug molecules. These spatially-resolved phenotypic changes contain functional molecular information associated with disease progression and drug action. Pharmacologists can evaluate drug efficacy by analyzing downstream metabolites that are regulated by the target enzyme or transporter. An untargeted spatial metabolomics study performed using MSI can also help to explore potential drug targets, screen the functional metabolite markers, and investigate the possible molecular mechanism.

The Agar group conducted a complementary analysis on the glioblastoma patient-derived xenograft (PDX) model. The erlotinib ion image was co-registered with the H&E staining, MRI, and immunohistochemistry (IHC) results to correlate the targeting distribution of the EGFR inhibitor, erlotinib, and resulting tumor phenotype changes, including phosphoproteomics, for assessing protein signaling response and mRNA sequencing for evaluating the transcriptional response. This comprehensive multi-omics information provides insight into pharmacokinetics/pharmacodynamics (PK/PD) correlation [82].

A hyperspectral imaging method was proposed to simultaneously monitor an anti-insomnia drug candidate, NHBA, and endogenous metabolic profile in whole-body rat sections by AFA-DESI-MSI [83]. The PCA-based hyperspectral imaging spatially revealed metabolic perturbation in response to the NHBA stimulation. Six functional metabolites were discovered to be significantly changed after drug intervention, including neurotransmitters (γ-aminobutyric acid, neurotransmitter precursors choline, and glycerophosphocholine), an endogenous sleep factor, adenosine, and creatine, which are closely associated with insomnia or other neurologic disorders (**Figure 5a**). These findings provide insight into the mechanism underlying NHBA action. It has also been shown that the power of MSI-based spatial metabolomics in studying the molecular mechanism of drug action, especially for drug candidates with multiple or undefined targets in the preclinical study stage. AFA-DESI-MSI combined with the metabolic network mapping method was developed to spatially-resolve the metabolic alterations from the micro-region of the rat brain. Key functional metabolites involved in the complex regulatory network in the central nervous system have been elucidated (**Figure 5b**) after intervention by scopolamine which is a drug candidate for treating Alzheimer's disease [84].

12. *IN VITRO* ACTIVITY EVALUATION AND HIGH THROUGHPUT SCREENING

In the early stage of drug discovery, hundreds of compounds were needed to go through *in vitro* high-throughput screening (HTS) to select small molecular hits with binding activity to the biological target before conducting the hit-to-lead (H2L) structural optimization and follow-up *in vitro* and *in vivo* DMPK studies. A qualified drug candidate should perform an ideal IC_{50} towards the target protein. This step requires a robust, and reliable *in vitro* evaluation method with a convenient signal readout system to reflect the compound's activity with varied chemical structures and test concentrations. In addition, the *in vitro* tested object should also be highly consistent among different batches to guarantee the comparability in compounds and reproducibility of the whole screening process. The traditional HTS system relies on the single signal readout system. In recent years, the use of MSI has also been put into more practice in the high-content HTS process because of label-free and multiplex detection.

The 2D media-cultured single cells are frequently used testing objects for *in vitro* activity evaluation and drug candidate screening. These cells contain stably- or transiently-expressed target protein (normally an enzyme, receptor, or transporter) through transfection. To characterize the cell uptake process, the cutting-edge MSI

©2022 The Authors. Creative Commons Attribution 4.0 International License

Acta Materia Medica

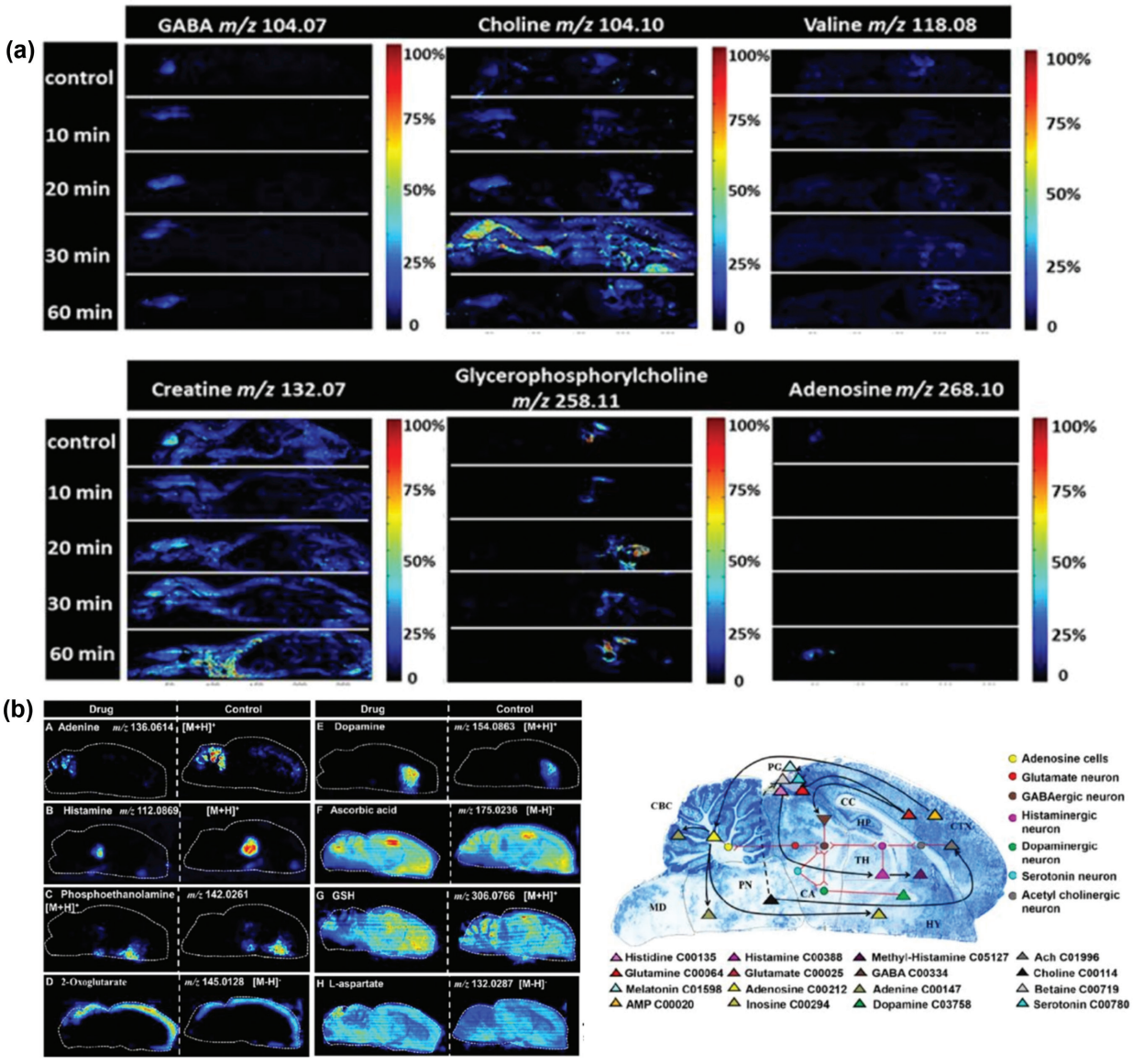

Figure 5 | Typical cases of MSI in a spatial pharmaco-metabolomics and molecular mechanism study.
(a) Spatiotemporal visualization of six endogenous metabolites in rat whole-body tissue sections after N^6-(4-hydroxybenzyl) adenine riboside (NHBA) treatment. Available on https://pubs.acs.org/doi/full/10.1021/acs.analchem.5b00680 and previously published in Ref. [83]; (b) Images of significantly changed metabolites in the sagittal brain sections and the metabolic network-based spatial correlation map. The control group presents rats modelled with learning and memory impairment. The drug group presents model rats treated with scopolamine [84]. Copyright 2021 *American Chemical Society*.

technique based on a laser or ion beam needs to be used to obtain the sub-cellular resolved drug ion image [15]. The Winograd group realized subcellular imaging of antibiotics in single *E. coli.* bacteria using time-of-flight secondary ion mass spectrometry (ToF-SIMS) with C_{60} cation as the ion beam. The spatial resolution reached 300 nm. The dose-response of ampicillin and tetracycline in *E. coli* cell aggregates was confirmed [12]. The Hang group developed a micro-lensed fiber (MLF) to focus the laser desorption post-ionization (LDPI) size to the 300 nm level [10]. Furthermore, the 3D distribution of two anti-tumor drugs, proflavine and methylthioninium chloride, within a single cell were realized at a voxel resolution of 500 × 500 × 500 nm^3 using micro-lensed fiber laser desorption post-ionization-mass spectrometry imaging [MLF-LDPI-MSI] (**Figure 6**) [85].

Recently, the 3D culturing-based organoids and tumor spheroids became a promising topic in the biomedical engineering field and gains the increasing interest of researchers. Unlike the 2D cultured cells, cells in the 3D organoid, and tumor spheroids have more similar topological structures as the native organ or tumor in the

©2022 The Authors. Creative Commons Attribution 4.0 International License

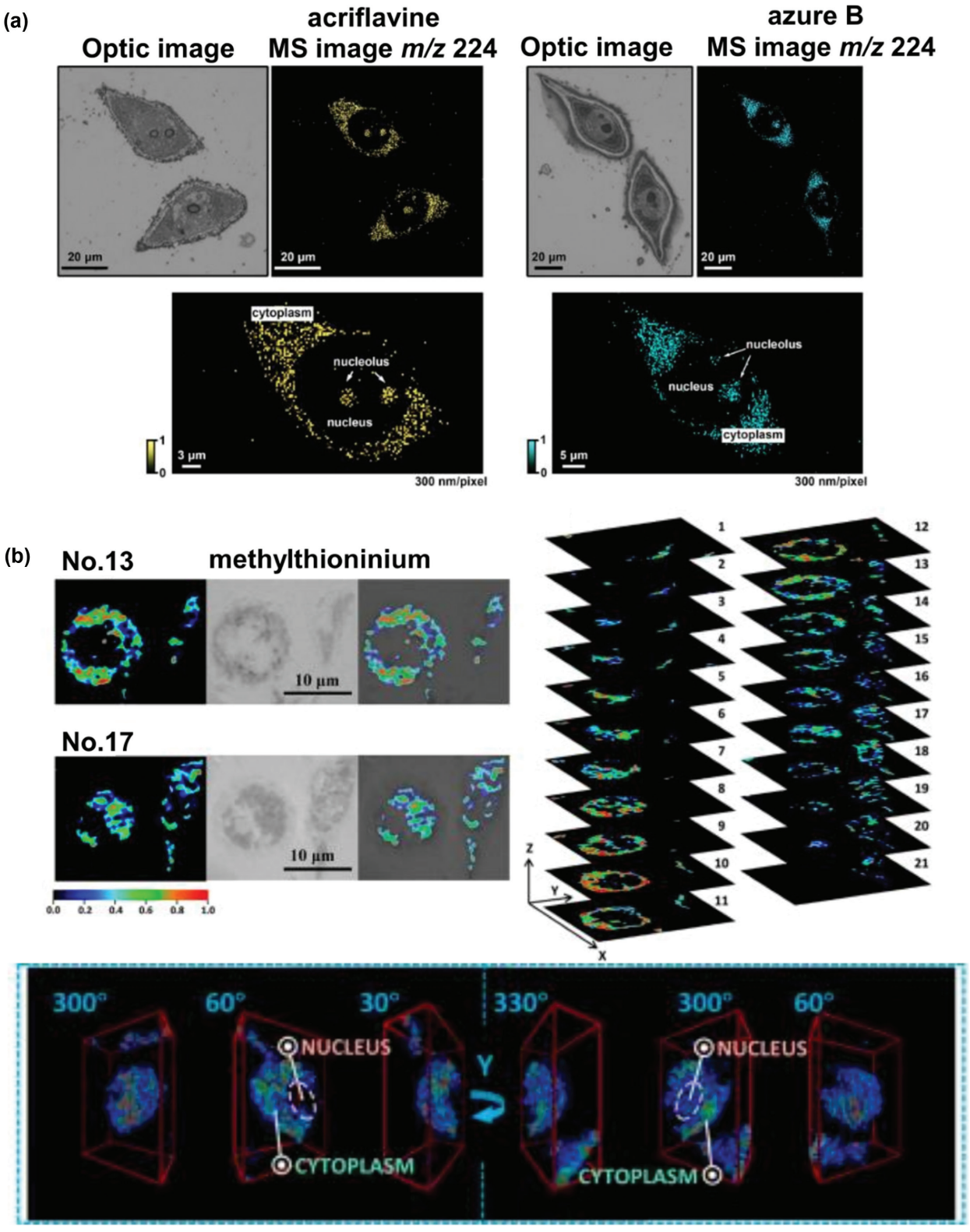

Figure 6 | Representative study cases for MSI application in the *in vitro* drug evaluation.
(a) The optical image, and MS image of single cells dosed with acriflavine and azure [10]; (b) 2D- and 3D images of methylthioninium chloride within a drug-treated HeLa cell [85].

©2022 The Authors. Creative Commons Attribution 4.0 International License

body because of the gradient nutrient supply and mass exchange with the external environment [86]. Paper becomes an emerging 3D culture medium because the microporous fiber structure can simulate the extracellular matrix (ECM) environment where endogenous cells live and grow. The potential of MALDI-MSI with paper-based 3D cell cultures has been demonstrated as a rapid, effective, and large-scale drug screening platform [87].

The Hummon group evaluated the penetration of doxorubicin-encased liposomes into 3D cell spheroids over the course of 72 h using MALDI-MSI combined with fluorescence microscopy. The free and liposomal doxorubicin, as well as its three active metabolites throughout the spheroids after 12 h of treatment, were identified [88]. Cho et. al constructed the self-assembling multicellular spheroids that have reproducible blood-brain barrier (BBB) features and functions for rapid screening of brain-penetrating drugs. The developed BBB spheroids were then successfully applied to the *ex vivo* transport of BKM120 (a BBB-penetrant drug) and dabrafenib (a non-penetrant drug) by MALDI-MSI [89]. Superhydrophobic–hydrophilic droplet microarrays (DMAs) were fabricated for the high-throughput cell assay platform for the purpose of MALDI-MSI-based high speed. The size of a spot in DMA was reduced to an internal diameter (ID) of 0.5 mm, allowing for as few as 10 A549 lung cancer cells confined in a 40-nL droplet for high-content drug profiling. Finally, a fatty acid synthase (FASN) inhibitor, GSK2194069, was successfully screened out as the drug candidate (**Figure 7**) [90].

13. SAFETY AND TOXICITY EVALUATION

Safety and toxicity tests are important items for assessing possible physiologic damage caused by a drug candidate in the preclinical trial. Many promising drug candidates may have to be suspended for further development because of the severe side effects or even toxicity. The side effects can be induced by the intensive or persistent dosing of the drug or the generation of a toxic metabolite. Special attention should be paid when the local accumulation of a drug in a non-target organ is observed, or its toxic metabolite is monitored. MSI cannot only provide the *in situ* evidence of the parent drug and its toxic metabolite accumulation, but also correlate the regional molecular profile with the histopathologic information, facilitating the molecular elucidation behind the side effect or toxicity on the impacted tissue region.

There is an increasing number of MSI application cases investigating organ accuracy and chronic toxicity, such as hepatotoxicity, nephrotoxicity [91], pulmonary toxicity [92], ocular toxicity, and neurotoxicity [93]. The Cai group integrated MALDI-MSI and MS-based lipidomics to study bisphenol S nephrotoxicity in mice after a 56-day long-term exposure. Glomerular necrosis in the renal cortex, cloudy swelling in the renal medulla, and interstitial collapsing in the renal pelvis were diagnosed. Dysfunctional lipids were those lipids which serve signaling, such as ceramide, sphingosine, and sphingomyelin, in the renal cortex, implicating the vulnerability of renal cortex lipids to the bisphenol S exposure than those in the renal medulla and pelvis [94]. Castellino *et al.* led a team in GlaxoSmithKline to investigate the metabolism and toxicity of an HIV non-nucleoside reverse transcriptase inhibitor, fosdevirine (FDV), in the central nervous system (CNS). The MALDI-MSI was applied to map the spatial pattern of FDV and its metabolites in the brains of rabbits, minipigs, and monkeys. A cysteine conjugate FDV metabolite was discovered to be the predominant component and persistent in the CNS for an extended period after the last dose in patients with seizure and minipigs. This metabolite was highly enriched in the white matter of rabbit and minipig brains, whereas the predominant component in monkey CNS was FDV, which was specifically located in the gray matter (**Figure 8a**) [95].

Organ toxicity after long-term or high-dose exposure to a drug can be tested on vertebrate models, such as rats, mice, minipigs, rabbits, and monkeys. In addition to these model animals, zebrafish, and its larvae or embryos are another important vertebrate model in genetics and toxicology (**Figure 8b**) [96, 97]. Shao *et al*. examined the distribution and metabolism of diazepam (DZP) and its chlorination disinfection byproduct, 2-methylamino-5-chlorobenzophenone (MACB), in zebrafish by DESI-MSI. MACB was shown to accumulate in the spinal cord of the female group. Thereafter, the enriched MACB also transversed through the BBB and induce microglial phagocytosis of neurons [98].

14. MSI FOR MEDICINAL PLANT AND NATURAL PRODUCT

Terrestrial and marine plants, along with their symbiotic microorganisms on earth, are the largest natural library containing abundant chemical species to be explored. The structural diversity of natural products provides a valuable molecular template for medicinal chemist optimization to satisfy the drug-like properties as a qualified lead compound [99]. MSI has shown its potential in localizing those previously known natural products within the active medicinal part of plants. Additionally, the MSI can also be used for differentiating the multiple steps for active natural product biosynthesis or monitoring the spatiotemporal chemical changes of active natural products during steaming or boiling process.

Compared to the extensively studied biological tissues, the MSI application in plant chemistry is still relatively lagging. In the author's personal view, the reason behind this phenomenon arises from several technical aspects. First, the natural product in a plant is also known as a secondary metabolite. They have a relatively

©2022 The Authors. Creative Commons Attribution 4.0 International License

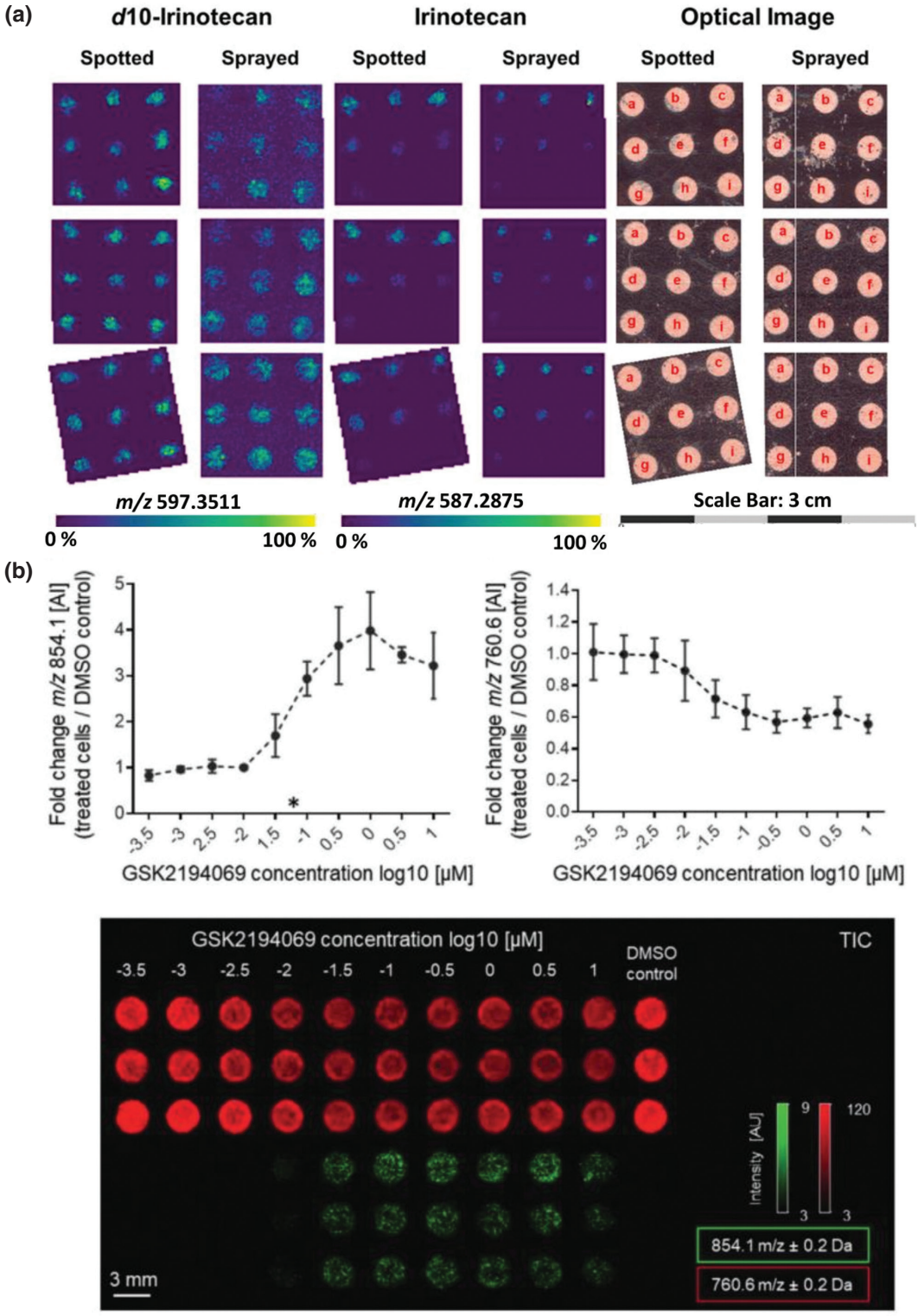

Figure 7 | *In vitro* cell-based high-throughput screening platforms built for MSI analysis.
(a) MALDI-MS images of irinotecan and its deuterated internal standard spotted or sprayed on the paper-based cell culturing scaffolds [87]; Copyright 2019 *American Chemical Society*. (b) Quantitative MALDI-MS imaging of the GSK20194069 response in A549 cancer cells on the droplet microarray platform. The fold-change (treated vs. control, n = 3) of endogenous malonyl-CoA (green spot) and PC (34:1) [red spot] in A549 cells was plotted against the inhibitor concentration. The IC_{50} is marked by an asterisk and derived from this concentration-response curve [90].

©2022 The Authors. Creative Commons Attribution 4.0 International License

Acta
Materia
Medica

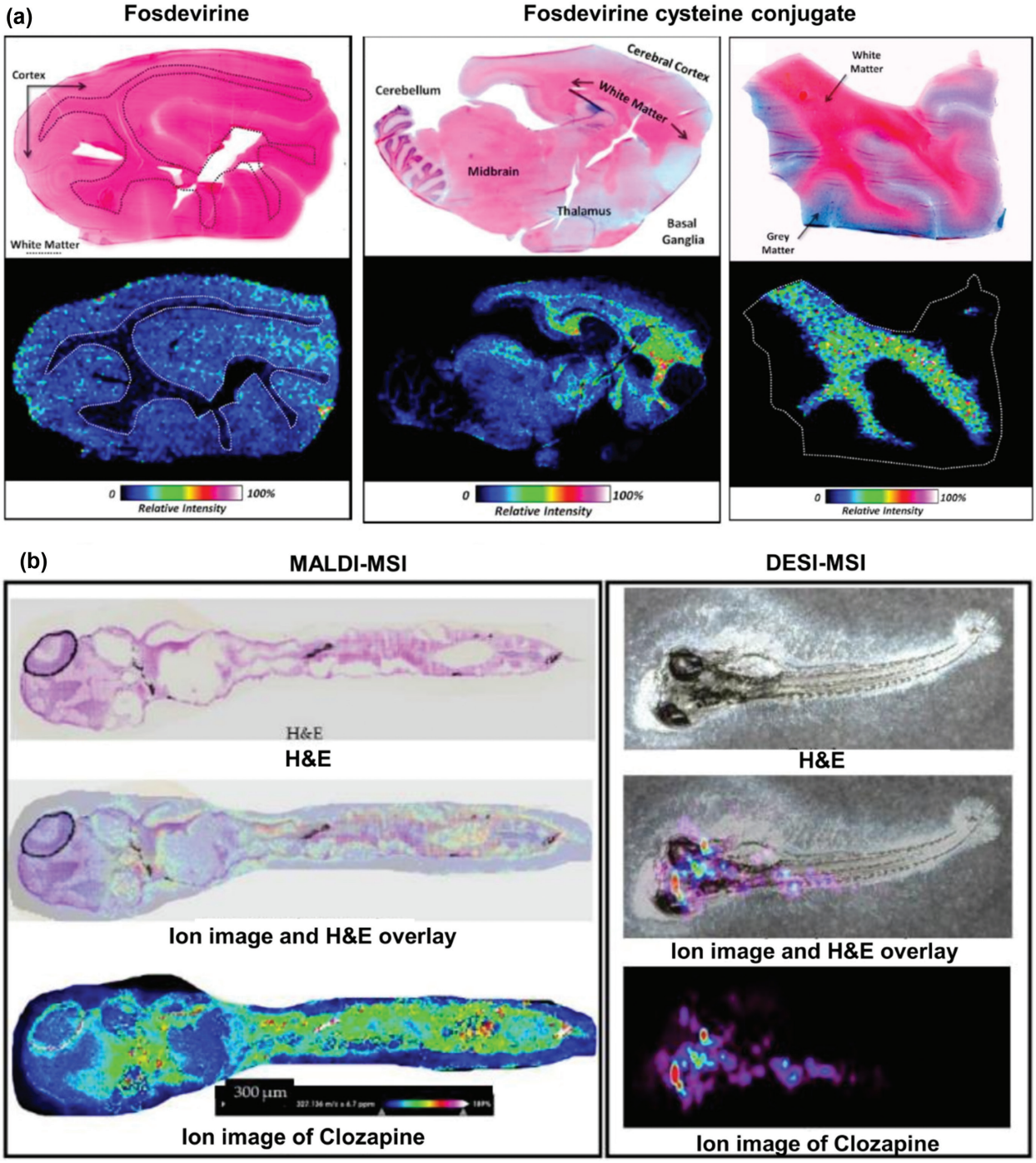

Figure 8 | Cases of MSI in drug safety and toxicity studies.
(a) Disposition and metabolism of fosdevirine (FDV) and its cysteine conjugate metabolite (M22) in the monkey (left), rabbit (middle), and minipig (right) sagittal brain sections. The left ion image mapped the FDV distribution and middle, right images mapped the M22 distribution; Copyright 2013 *American Chemical Society*. Adapted with permission from reference [95]. (b) Clozapine ion images in dosed zebrafish larvae acquired by MALDI (left) and DESI (right) [97].

low content compared to the universally existing primary metabolites, such as amino acids, lipids, carbohydrates, and nucleotides. The more potent a natural product, the less content existing within a plant/microorganism. Second, a plant cell has a unique cellulose wall providing hydrophobic mechanic protection. It

©2022 The Authors. Creative Commons Attribution 4.0 International License

is not as easy as a biological tissue for sectioning and adhesively mounted on the substrate for MSI analysis. Third, the availability of plant metabolomics databases is still short in hand for a confident assignment of detectable species from plant imaging. In most situations, natural products derived from a certain type of parent structure are isomers with the only positional difference in substitute groups. The identity of an ion is still hard to accurately assign without the aid of LC-MS/MS or nuclear magnetic resonance (NMR) as complementary. All these reasons pose a methodologic challenge in sensitive detection and accurate structural identification by MSI.

Nevertheless, technical improvement efforts have been made to address these putative issues, including the development of nanomaterials for plant imprinting and on-tissue chemical derivatization of natural products with a specific functional group. A new composite substrate, a hydrophobic polydopamine-modified TiO_2 nanotube coated with plasmonic gold nanoparticle, was constructed as a dual-polarity surface-assisted laser desportion/ionization (SALDI) substrate. The intricate structural details of plant samples can be preserved and transferred for the MSI study. The flavonoids, coumarins, and anti-tumor medicine, vinblastine, were successfully visualized from the imprinted petal of *J. integerrima* [100] (**Figure 9a**).

Apart from the method development for plant imaging, there were also mounting reports of MSI in evaluating the *in vivo* isolated natural product properties and a localization study [101]. The MSI application for the *in vivo* structure-activity relationship (SAR) of natural products has been reported recently. The Guo group quantitatively evaluated the distribution of 7 monoterpene indole alkaloids in 13 rat brain microcompartments by DESI-MSI. These alkaloids were isolated from *Uncaria* species (Rubiaceae), a traditional Chinese medicine (TCM) for treating CNS diseases. The distribution trend of these *Uncaria* alkaloids and the R/S-configuration epimer influence were summarized to provide valuable SAR information [102]. Sun *et al.* used MALDI-MSI to successfully map distributions of notoginsenoside-R1, notoginsenoside-Fc, ginsenoside-Re in the rhizome, and root of *Panax notoginseng* (**Figure 9b**), a highly valuable herbal medicine used in Asian for the treatment of cardiovascular and hematologic diseases. Furthermore, the spatiotemporal changes during the 2 h steaming process. Series of metabolites were also discovered to significantly change by streaming (**Figure 9c-d**) [103]. Kusari and Spiteller collaboratively reported the use of MALDI-MSI in probing several maytansinoids (maytansine, maytanprine, maytanbutine, maytanvaline, and normaytancyprine) distribution in Putterlickia pyracantha plants. These active maytansinoids show remarkable antibiotic activities along with high cytotoxicity. Many of the maytansinoids have been put into the front line of chemotherapy or clinical trials for treating breast cancer [104].

The spatially-resolved biosynthesis pathway for the active natural product is another important field for plant chemistry. Qiu and Chen studied the spatial distributions of phenolic acids, flavonoids, and tanshinones across the underground and aerial parts of *Salvia miltiorrhiza*. The flavonoids and phenolic acids were chosen for in-depth visualization of phenylpropanoid biosynthesis pathways in *S. miltiorrhiza*. DESI-MSI highlighted key reactions of flavonoid biosynthesis in flowers and identified the core precursor for phenolic acid biosynthesis in *Salvia* species [105].

15. PROSPECTIVE OUTLOOK

MSI has been shown to be a powerful tool in pharmaceutical research at the preclinical and clinical phases. Nonetheless, MSI still has room for further improvement in technique and methodology. The technical advances in MSI and its application in pharmaceutical research are summarized in **Figure 10** for an overview to what extent MSI has been developed in the two decades of common efforts by the whole community, and which specific research topics MSI is still poorly investigated and unsolved in future. The author would like to share some personal viewpoints on the direction in which the MSI can be further developed as a better multiplex molecular imaging technique.

1. Sensitivity: A more sensitive *in situ* soft ionization method needs to be further developed to acquire molecular profile, even from the sub-micron-sized impact region without severe loss in sensitivity. Efforts should be continuously made in the following: the novel sample-mounting nanomaterials; well-designed secondary-ionization; intricate ion focusing lens system; sample-friendly pre-processing; and chemical derivatization. This is always a critical research field that may drive the entire MSI research community forward. The territory of applicable pharmaceutical research will also be expanded due to the technical advancement.

2. Spatial resolution: This is another critical MSI metric to determine how precise an ion image can be acquired to learn more detailed spatial information. In most situations, this is a paradox issue conjugating with the sensitivity because a smaller sampling size usually means a very limited molecular amount and the corresponding signal response given a constant ionization efficiency. Currently, spatial resolution improvement can be achieved by a multi-modular image fusion strategy. Molecular information in a smaller region can be predicted by co-registering pixels from a rough MS image with other cell-resolved digital images acquired from H&E, IF, and MRI, [70, 75, 106, 107]. This high-resolution image is artificially predicted other than being really observed. Once soft ionization gains another evolutionary breakthrough in sensitivity,

©2022 The Authors. Creative Commons Attribution 4.0 International License

Acta Materia Medica

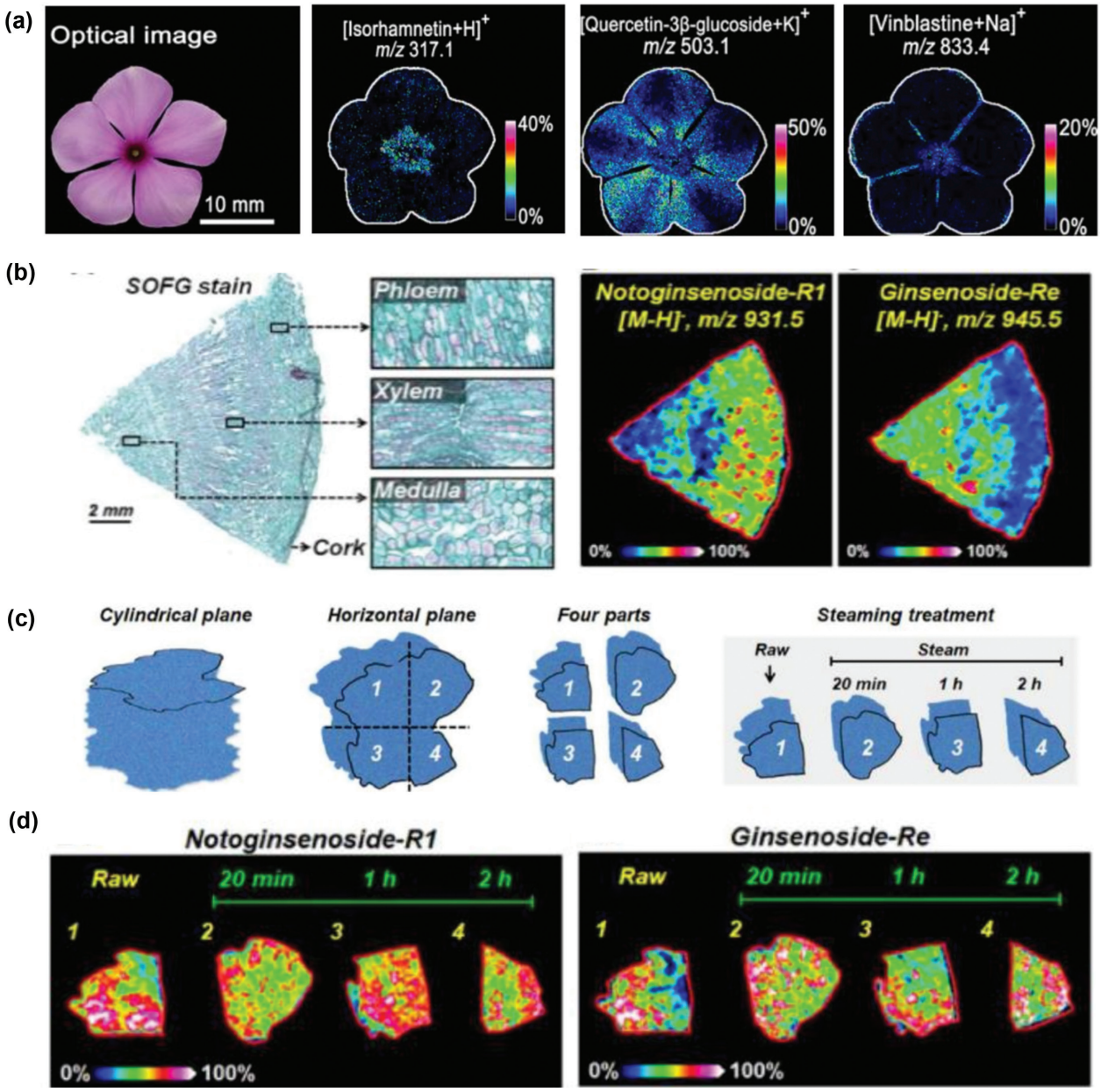

Figure 9 | Representative cases of MSI application in medicinal plant chemistry.
(a) Localization of isorhamnetin, quercetin-3β-glucoside, and an anti-tumor cytotoxic drug vinblastine across the imprinted petal of *J. integerrima*; Copyright 2022 *American Chemical Society*. Adapted with permission from reference [133]. (b) Differentiated distributions of notoginsenoside-R1 and ginsenoside-Re in the *P. notoginseng* root section; (c) The raw and steam-processed *P. notoginseng* tissues from same *P. notoginseng* root.; (d) Contents and distributions of notoginsenoside-R1 and ginsenoside-Re during the streaming process. Copyright 2021 *The Korean Society of Ginseng*. Adapted with permission from reference [103].

a more universe, cost-effective MSI method for sub-micron-resolved drug/metabolite imaging will not be the bottleneck for the single-cell, spatial phenotypic-omics.

3. Coverage of detectable species: MSI is expected to be a universally-applicable molecular imaging method to all types of functional proteins, glycans, metabolites, and drugs. Thus, the complex networks consisting of all molecules for signaling regulation, metabolism, and interaction can be spatiotemporally explored. From the of proteomic imaging, especially for those protein complexes or membrane proteins, although there have been

©2022 The Authors. Creative Commons Attribution 4.0 International License

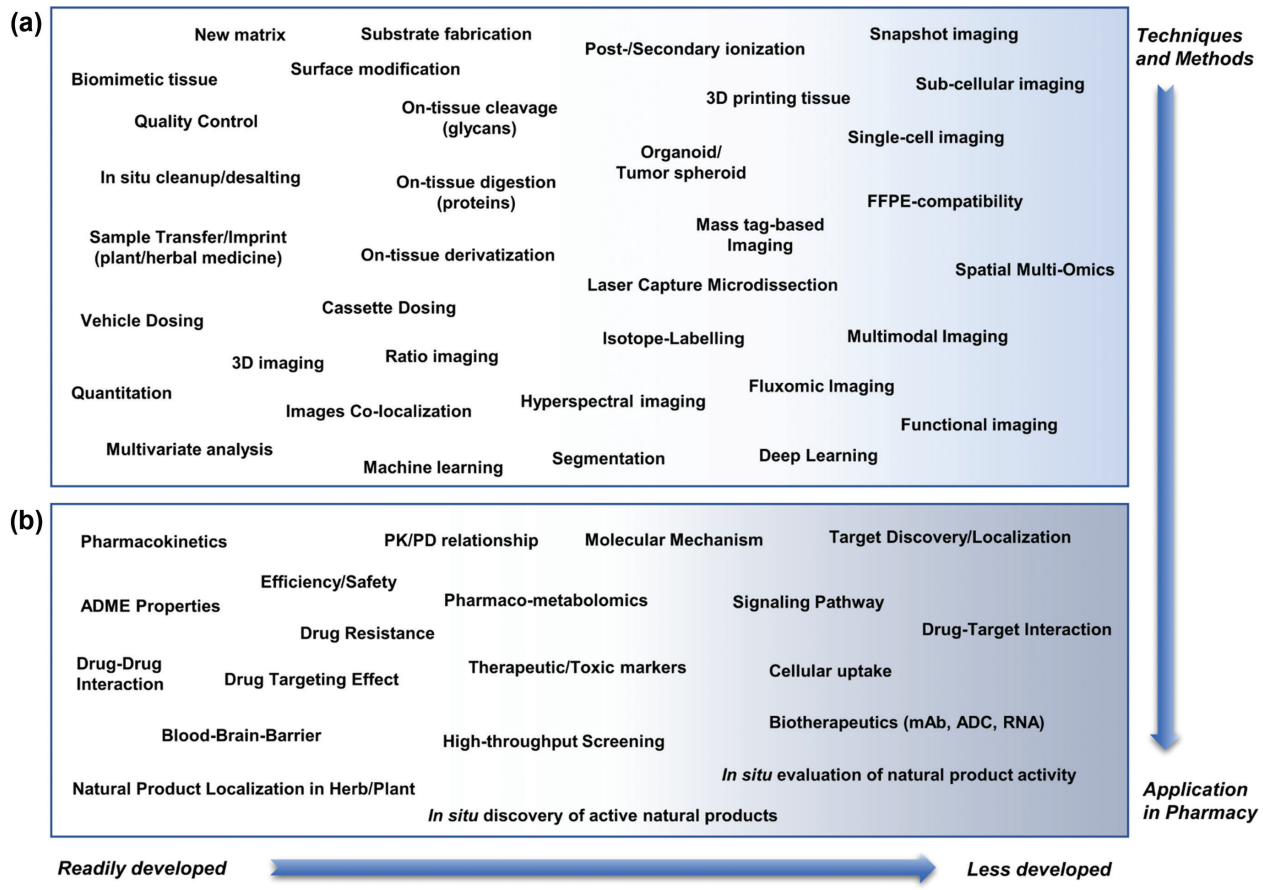

Figure 10 | Retrospective overview and prospective outlook of MSI technique advances and its application in pharmaceutical research.

(a) MSI technique advancement; (b) Reported MSI application in pharmacy. Fields close to the left side are those which have been relatively well-developed and fields more closer to the right side are those which remained less developed.

native MSI methods proposed for direct detection of those functional membrane proteins or complexes [108, 109], the mass tag-based ionization and imaging provide a feasible and universal strategy to indirectly report the locations for these functional macromolecules [110-114]. Thus far, compared to the small molecular drugs, the, such as monoclonal antibody drug (mAb), antibody-drug conjugate (ADC), and RNA drugs, still lack reports in the MSI field.

4. Diversity of testable objects: The biospecimens for MSI study have widely covered the whole-body animal sections from rats, mice, minipigs, zebrafish, monkeys, tumor spheroids, and xenografted tumors from model animals or patients, fragile organs like lungs, and eye lenses, cultured single cells, and 3D organoids. An way to make MSI compatible with the formalin-fixed paraffin embedding tissue sections is limited, and more widely used biospecimens in clinical pathology, particularly for ambient ionization-based drug/metabolomics imaging studies.

5. Data collection mode: An industrialized robot system for automatic management of batch tissue samples, streamlined MSI data acquisition, and quality control is expected to establish a more standardized procedure. It is surprising to notice that effort has been made in this industrial design direction [115]. Currently, the microprobe-based spot-by-spot or line-by-line scan mode remains the predominant way for MSI data collection, which usually takes hours or even a whole day to complete for a larger size sample or when the ultrahigh-resolution image is required. A rapid, microscopic snapshot-mode MSI data collection will definitely accelerate the MSI working efficiency [116]. This requires a more sophisticated MS instrumentation design in the micro-arrayed ion detection system.

6. Isobaric ion differentiation and reliable identification: MSI has the difficulty in recognizing isobaric ions due to the *in situ* detection principle. Ions with identical formula composition cannot be differentiated. The invention of ion mobility mass

©2022 The Authors. Creative Commons Attribution 4.0 International License

spectrometry (IMS) provides a feasible direction to overcome this limitation because it actually plays a role in gas-phase ion "chromatography" separation. The separating ability is still under further improvement. Ion identification is another issue posed to the MSI method. A relatively confident result for an ion identification could be assured by chemometrics based on multiple matching criteria, including exact mass tolerance, isotope abundance, adduct ion types, and featured fragments [117-119]. Apart from the post-acquisition dry method, the online wet experiments also provide complementary chemical structure to help isobaric ion differentiation, such as hydrogen-deuterium exchange (HDX) during the ionization process in the liquid phase or and post-ionization traveling process in the gas phase [120, 121].

7. Functional Imaging: Mass spectral profile acquired by an MSI experiment is not simply the list of separated irrelevant peaks; there are biological connections among these peaks. These bio-informative connections could provide insight into the drug-phenotype interaction, and spatially resolved molecular composition-environment-biological function. It is believed that MSI can also become a functional imaging tool to visualize biological events, such as proliferation, metastasis, invasion, autophagy, ferroptosis [122, 123], and biomolecular activity, such as enzyme catalysis [124-127], and biological tissue microenvironments, such as acidity [128], by analyzing and organizing the acquired big data.

8. Artificial intelligence: Deep learning has already been introduced to learn the molecular profile pattern and guide precise spatial recognition [39]. It is expected to introduce more cutting-edge data science techniques and computation methods to facilitate the integration of spatial multi-omics information, such as spatial genomics and transcriptomics.

9. Open-access to spatial omics database or platform: An open-access MSI data platform should be proposed and encouraged for MSI researchers' free exploration and communication [129]. It is also expected for an open-access spatial omics database containing molecular phenotype atlas from key organs and cancer tissue. This, of course, needs the common efforts and consensus of the entire MSI and spatial omics community. It is critical not only for the MSI community, but also for multimodality imaging analysis between MS images and other molecular imaging techniques for the entire spatial omics community.

ACKNOWLEDGEMENTS

The author would like to acknowledge the support of the National Natural Science Foundation of China (No. 81903575) during his research period at Fudan University.

CONFLICTS OF INTERESTS

The authors state no competing interest with any academic institute or industry.

REFERENCES

[1] Nilsson A, Goodwin RJ, Shariatgorji M, Vallianatou T, Webborn PJ, Andren PE: Mass Spectrometry Imaging in Drug Development. *Analytical Chemistry* 2015, 87:1437–1455.
[2] Goodwin RJA, Takats Z, Bunch J: A Critical and Concise Review of Mass Spectrometry Applied to Imaging in Drug Discovery. *SLAS Discovery: Advancing Life Sciences R & D* 2020, 25:963–976.
[3] Prideaux B, Stoeckli M: Mass Spectrometry Imaging for Drug Distribution Studies. *Journal of Proteomics* 2012, 75:4999–5013.
[4] Stoeckli M, Staab D, Schweitzer A: Compound and Metabolite Distribution Measured by MALDI Mass Spectrometric Imaging in Whole-body Tissue Sections. *International Journal of Mass Spectrometry* 2007, 260:195–202.
[5] Cooks RG, Ouyang Z, Takats Z, Wiseman JM: Detection Technologies. Ambient Mass Spectrometry. *Science* 2006, 311:1566–1570.
[6] Wiseman JM, Ifa DR, Song Q, Cooks RG: Tissue Imaging at Atmospheric Pressure Using Desorption Electrospray Ionization (DESI) Mass Spectrometry. *Angewandte Chemie* (*International Ed In English*) 2006, 45:7188–7192.
[7] Feider CL, Krieger A, DeHoog RJ, Eberlin LS: Ambient Ionization Mass Spectrometry: Recent Developments and Applications. *Analytical Chemistry* 2019, 91:4266–4290.
[8] Wu V, Tillner J, Jones E, McKenzie JS, Gurung D, Mroz A, et al.: High Resolution Ambient MS Imaging of Biological Samples by Desorption Electro-Flow Focussing Ionization. *Analytical Chemistry* 2022, 94:10035–10044.
[9] Huang J, Gao S, Wang K, Zhang J, Pang X, Shi J, et al.: Design and Characterizing of Robust Probes for Enhanced Mass Spectrometry Imaging and Spatially Resolved Metabolomics. *Chinese Chemical Letters* 2022:107865.
[10] Meng Y, Cheng X, Wang T, Hang W, Li X, Nie W, et al.: Micro-Lensed Fiber Laser Desorption Mass Spectrometry Imaging Reveals Subcellular Distribution of Drugs within Single Cells. *Angewandte Chemie* (*International Ed In English*) 2020, 132:18020–18027.
[11] Niehaus M, Soltwisch J, Belov ME, Dreisewerd K: Transmission-Mode MALDI-2 Mass Spectrometry Imaging of Cells and Tissues at Subcellular Resolution. *Nature Methods* 2019, 16:925–931.
[12] Tian H, Six DA, Krucker T, Leeds JA, Winograd N: Subcellular Chemical Imaging of Antibiotics in Single Bacteria Using C60-Secondary Ion Mass Spectrometry. *Analytical Chemistry*. 2017, 89:5050–5057.
[13] Tian H, Sparvero LJ, Blenkinsopp P, Amoscato AA, Watkins SC, Bayır H, et al.: Secondary-Ion Mass Spectrometry Images Cardiolipins and Phosphatidylethanolamines at the Subcellular Level. *Angewandte Chemie* (*International Ed In English*) 2019, 58:3156–3161.
[14] Song X, Chen H: Desorption Electrospray Ionization Mass Spectrometry Imaging for Tissue Analysis. In *Encyclopedia of Analytical Chemistry*, Meyers RA (Ed.). 2020:1–45. https://doi.org/10.1002/9780470027318.a9640.
[15] Wang T, Cheng X, Xu H, Meng Y, Yin Z, Li X, et al.: Perspective on Advances in Laser-Based High-Resolution

©2022 The Authors. Creative Commons Attribution 4.0 International License

Mass Spectrometry Imaging. *Analytical Chemistry* 2020, 92:543–553.
[16] Buchberger AR, DeLaney K, Johnson J, Li L: Mass Spectrometry Imaging: A Review of Emerging Advancements and Future Insights. *Analytical Chemistry* 2018, 90:240–265.
[17] Chumbley CW, Reyzer ML, Allen JL, Marriner GA, Via LE, Barry CE, et al.: Absolute Quantitative MALDI Imaging Mass Spectrometry: A Case of Rifampicin in Liver Tissues. *Analytical Chemistry*. 2016, 88:2392–2398.
[18] Liu C, Qi K, Yao L, Xiong Y, Zhang X, Zang J, et al.: Imaging of Polar and Nonpolar Species Using Compact Desorption Electrospray Ionization/Postphotoionization Mass Spectrometry. *Analytical Chemistry* 2019, 91:6616–6623.
[19] Soltwisch J, Kettling H, Vens-Cappell S, Wiegelmann M, Müthing J, Dreisewerd K: Mass Spectrometry Imaging with Laser-Induced Postionization. *Science* 2015, 348:211–215.
[20] He J, Tang F, Luo Z, Chen Y, Xu J, Zhang R, et al.: Air Flow Assisted Ionization for Remote Sampling of Ambient Mass Spectrometry and Its Application. *Rapid Communications in Mass Spectrometry* 2011, 25:843–850.
[21] He J, Sun C, Li T, Luo Z, Huang L, Song X, et al.: A Sensitive and Wide Coverage Ambient Mass Spectrometry Imaging Method for Functional Metabolites Based Molecular Histology. *Advanced Science* 2018, 5:1800250.
[22] Sun C, Liu W, Mu Y, Wang X: 1,1′-Binaphthyl-2,2′-diamine As a Novel MALDI Matrix to Enhance the In Situ Imaging of Metabolic Heterogeneity in Lung Cancer. *Talanta*. 2020, 209:120557.
[23] Niziol J, Ossolinski K, Ossolinski T, Ossolińska A, Bonifay V, Sekuła J, et al.: Surface-Transfer Mass Spectrometry Imaging of Renal Tissue on Gold Nanoparticle Enhanced Target. *Analytical Chemistry* 2016, 88:7365–7371.
[24] Sun C, Liu W, Geng Y, Wang X: On-Tissue Derivatization Strategy for Mass Spectrometry Imaging of Carboxyl-Containing Metabolites in Biological Tissues. *Analytical Chemistry* 2020, 92:12126–12131.
[25] Ma Z, Yuan J, Xu J, Li L, Tang C, Chang L, et al.: Quaternized Acridine Maleimide MALDI Probe Enables Mass Spectrometry Imaging of Thiols. *Analytical Chemistry* 2022, 94:14917–14924.
[26] Barre FP, Flinders B, Garcia JP, Jansen I, Huizing LRS, Porta T, et al.: Derivatization Strategies for the Detection of Triamcinolone Acetonide in Cartilage by Using Matrix-Assisted Laser Desorption/Ionization Mass Spectrometry Imaging. *Analytical Chemistry* 2016, 88:12051–12059.
[27] Wu Q, Comi TJ, Li B, Rubakhin SS, Sweedler JV: On-Tissue Derivatization via Electrospray Deposition for Matrix-Assisted Laser Desorption/Ionization Mass Spectrometry Imaging of Endogenous Fatty Acids in Rat Brain Tissues. *Analytical Chemistry* 2016, 88:5988–5995.
[28] Han Y, Zhao Y, Chen P, Wang L, Hu Q, Wang X, et al.: On-tissue Derivatization for Isomer-specific Mass Spectrometry Imaging and Relative Quantification of Monosaccharides in Biological Tissues. *Analytica Chimica Acta* 2022, 1225:340241.
[29] Sun C, Li Z, Ma C, Zang Q, Li J, Liu W, et al.: Acetone Immersion Enhanced MALDI-MS Imaging of Small Molecule Metabolites in Biological Tissues. *Journal of Pharmaceutical and Biomedical Analysis* 2019, 176:112797.
[30] Shariatgorji M, Kallback P, Gustavsson L, Schintu N, Svenningsson P, Goodwin RJ, et al.: Controlled-pH Tissue Cleanup Protocol for Signal Enhancement of Small Molecule Drugs Analyzed by MALDI-MS Imaging. *Analytical Chemistry* 2012, 84:4603–4607.
[31] Song X, Luo Z, Li X, Li T, Wang Z, Sun C, et al.: In Situ Hydrogel Conditioning of Tissue Samples to Enhance the Drug's Sensitivity in Ambient Mass Spectrometry Imaging. *Analytical Chemistry* 2017, 89:6318–6323.
[32] Lamont L, Eijkel GB, Jones EA, Flinders B, Ellis SR, Siegel TP, et al.: Targeted Drug and Metabolite Imaging: Desorption Electrospray Ionization Combined with Triple Quadrupole Mass Spectrometry. *Analytical Chemistry* 2018, 90:13229–13235.
[33] Niziol J, Sunner J, Beech I, Ossoliński K, Ossolińska A, Ossoliński T, et al.: Localization of Metabolites of Human Kidney Tissue with Infrared Laser-Based Selected Reaction Monitoring Mass Spectrometry Imaging and Silver-109 Nanoparticle-Based Surface Assisted Laser Desorption/Ionization Mass Spectrometry Imaging. *Analytical Chemistry* 2020, 92:4251–4258.
[34] Garza KY, Feider CL, Klein DR, Rosenberg JA, Brodbelt JS, Eberlin LS: Desorption Electrospray Ionization Mass Spectrometry Imaging of Proteins Directly from Biological Tissue Sections. *Analytical Chemistry*. 2018, 90:7785–7789.
[35] Djambazova KV, Klein DR, Migas LG, Neumann EK, Rivera ES, Van de Plas R, et al.: Resolving the Complexity of Spatial Lipidomics Using MALDI TIMS Imaging Mass Spectrometry. *Analytical Chemistry* 2020, 92:13290–13297.
[36] Robbe MF, Both JP, Prideaux B, Klinkert I, Picaud V, Schramm T, et al.: Software tools of the Computis European Project to Process Mass Spectrometry Images. *European Journal of Mass Spectrometry* 2014, 20:351–360.
[37] Hu H, Laskin J: Emerging Computational Methods in Mass Spectrometry Imaging. *Advanced Science* 2022, 9:e2203339.
[38] Guo L, Hu Z, Zhao C, Xu X, Wang S, Xu J, et al.: Data Filtering and Its Prioritization in Pipelines for Spatial Segmentation of Mass Spectrometry Imaging. *Analytical Chemistry* 2021, 93:4788–4793.
[39] Guo L, Liu X, Zhao C, Hu Z, Xu X, Cheng K-K, et al.: iSegMSI: An Interactive Strategy to Improve Spatial Segmentation of Mass Spectrometry Imaging Data. *Analytical Chemistry* 2022, 94:14522–14529.
[40] Fonville JM, Carter CL, Pizarro L, Steven RT, Palmer AD, Griffiths RL, et al.: Hyperspectral Visualization of Mass Spectrometry Imaging Data. *Analytical Chemistry* 2013, 85:1415–1423.
[41] Yang J, Rubel O, Prabhat, Mahoney MW, Bowen BP: Identifying Important Ions and Positions in Mass Spectrometry Imaging Data using CUR Matrix Decompositions. *Analytical Chemistry* 2015, 87: 4658–4666.
[42] McDonnell LA, van Remoortere A, de Velde N, van Zeijl RJ, Deelder AM: Imaging Mass Spectrometry Data Reduction: Automated Feature Identification and Extraction. *Journal of the American Society for Mass Spectrometry* 2010, 21:1969–1978.
[43] Song X, He J, Pang X, Zhang J, Sun C, Huang L, et al.: Virtual Calibration Quantitative Mass Spectrometry Imaging for Accurately Mapping Analytes across Heterogenous Biotissue. *Analytical Chemistry* 2019, 91:2838–2846.
[44] Seeley EH, Caprioli RM: 3D Imaging by Mass Spectrometry: A New Frontier. *Analytical Chemistry* 2012, 84: 2105–2110.
[45] Klinkert I, Chughtai K, Ellis SR, Heeren RMA: Methods for Full Resolution Data Exploration and Visualization for Large 2D and 3D Mass Spectrometry Imaging Datasets. *International Journal of Mass Spectrometry* 2014, 362: 40–47.

©2022 The Authors. Creative Commons Attribution 4.0 International License

[46] Duncan KD, Lanekoff I: Oversampling to Improve Spatial Resolution for Liquid Extraction Mass Spectrometry Imaging. *Analytical Chemistry* 2018, 90:2451–2455.
[47] Hu H, Helminiak D, Yang M, Unsihuay D, Hilger RT, Ye DH, et al.: High-Throughput Mass Spectrometry Imaging with Dynamic Sparse Sampling. *ACS Measurement Science Au* 2022, 2:466–474.
[48] Abdelmoula WM, Skraskova K, Balluff B, Carreira RJ, Tolner EA, Lelieveldt BPF, et al.: Automatic Generic Registration of Mass Spectrometry Imaging Data to Histology Using Nonlinear Stochastic Embedding. *Analytical Chemistry* 2014, 86:9204–9211.
[49] Abdelmoula WM, Carreira RJ, Shyti R, Balluff B, van Zeijl RJM, Tolner EA, et al.: Automatic Registration of Mass Spectrometry Imaging Data Sets to the Allen Brain Atlas. *Analytical Chemistry* 2014, 86:3947–3954.
[50] Norris JL, Farrow MA, Gutierrez DB, Palmer LD, Muszynski N, Sherrod SD, et al.: Integrated, High-Throughput, Multiomics Platform Enables Data-Driven Construction of Cellular Responses and Reveals Global Drug Mechanisms of Action. *Journal of Proteome Research* 2017, 16:1364–1375.
[51] Denti V, Capitoli G, Piga I, Clerici F, Pagani L, Criscuolo L, et al.: Spatial Multiomics of Lipids, N-Glycans, and Tryptic Peptides on a Single FFPE Tissue Section. *Journal of Proteome Research* 2022, 21:2798–2809.
[52] Pirman DA, Kiss A, Heeren RM, Yost RA: Identifying Tissue-specific Signal Variation in MALDI Mass Spectrometric Imaging by Use of an Internal Standard. *Analytical Chemistry* 2013, 85:1090–1096.
[53] Taylor AJ, Dexter A, Bunch J: Exploring Ion Suppression in Mass Spectrometry Imaging of a Heterogeneous Tissue. *Analytical Chemistry* 2018, 90:5637–5645.
[54] Mohammadi S, Parastar H: Quantitative Analysis of Multiple High-Resolution Mass Spectrometry Images Using Chemometric Methods: Quantitation of Chlordecone in Mouse Liver. *Analyst* 2018, 143:2416–2425.
[55] Luo Z, He J, He J, Huang L, Song X, Li X, et al.: Quantitative Analysis of Drug Distribution by Ambient Mass Spectrometry Imaging Method with Signal Extinction Normalization Strategy and Inkjet-Printing Technology. *Talanta* 2018, 179:230–237.
[56] Pirman DA, Reich RF, Kiss A, Heeren RM, Yost RA: Quantitative MALDI Tandem Mass Spectrometric Imaging of Cocaine from Brain Tissue with a Deuterated Internal Standard. *Analytical Chemistry* 2013, 85:1081–1089.
[57] Landgraf RR, Garrett TJ, Conaway MC, Calcutt NA, Stacpoole PW, Yost RA: Considerations for Quantification of Lipids in Nerve Tissue Using Matrix-Assisted Laser Desorption/Ionization Mass Spectrometric Imaging. *Rapid Communications in Mass Spectrometry* 2011, 25:3178–3184.
[58] Groseclose MR, Castellino S: A Mimetic Tissue Model for the Quantification of Drug Distributions by MALDI Imaging Mass Spectrometry. *Analytical Chemistry* 2013, 85:10099–10106.
[59] Song X, He J, Li C, Sun C, Pang X, Zhang J, et al.: Fabrication of Homogenous Three-dimensional Biomimetic Tissue for Mass Spectrometry Imaging. *Journal of Mass Spectrometry* 2019, 54:378–388.
[60] Cahill JF, Kertesz V, Weiskittel TM, Vavrek M, Freddo C, Van Berkel GJ: Online, Absolute Quantitation of Propranolol from Spatially Distinct 20- and 40-μm Dissections of Brain, Liver, and Kidney Thin Tissue Sections by Laser Microdissection-Liquid Vortex Capture-Mass Spectrometry. *Analytical Chemistry* 2016, 88:6026–6034.
[61] Dilillo M, Pellegrini D, Ait-Belkacem R, de Graaf EL, Caleo M, McDonnell LA: Mass Spectrometry Imaging, Laser Capture Microdissection, and LC-MS/MS of the Same Tissue Section. *Journal of Proteome Research* 2017, 16:2993–3001.
[62] Swales JG, Tucker JW, Strittmatter N, Nilsson A, Cobice D, Clench MR, et al.: Mass Spectrometry Imaging of Cassette-Dosed Drugs for Higher Throughput Pharmacokinetic and Biodistribution Analysis. *Analytical Chemistry* 2014, 86:8473–8480.
[63] Liu X, Ide JL, Norton I, Marchionni MA, Ebling MC, Wang LY, et al.: Molecular Imaging of Drug Transit Through the Blood-Brain Barrier with MALDI Mass Spectrometry Imaging. *Scientific Reports* 2013, 3:2859.
[64] Prasad M, Postma G, Franceschi P, Buydens LMC, Jansen JJ: Evaluation and Comparison of Unsupervised Methods for the Extraction of Spatial Patterns from Mass Spectrometry Imaging Data (MSI). *Scientific Reports* 2022, 12:15687.
[65] Lin LE, Chen CL, Huang YC, Chung H-H, Lin C-W, Chen K-C, et al.: Precision Biomarker Discovery Powered by Microscopy Image Fusion-assisted High Spatial Resolution Ambient Ionization Mass Spectrometry Imaging. *Analytica Chimica Acta* 2020, 1100:75–87.
[66] Cahill JF, Kertesz V, Van Berkel GJ: Characterization and Application of a Hybrid Optical Microscopy/Laser Ablation Liquid Vortex Capture/Electrospray Ionization System for Mass Spectrometry Imaging with Sub-micrometer Spatial Resolution. *Analytical Chemistry* 2015, 87:11113–11121.
[67] Tata A, Gribble A, Ventura M, Ganguly M, Bluemke E, Ginsberg HJ, et al.: Wide-field Tissue Polarimetry Allows Efficient Localized Mass Spectrometry Imaging of Biological Tissues. *Chemical Science* 2016, 7:2162–2169.
[68] Woolman M, Gribble A, Bluemke E, Zou J, Ventura M, Bernards N, et al.: Optimized Mass Spectrometry Analysis Workflow with Polarimetric Guidance for Ex Vivo and In Situ Sampling of Biological Tissues. *Scientific Reports* 2017, 7:468.
[69] Martin-Saiz L, Mosteiro L, Solano-Iturri JD, Rueda Y, Martín-Allende J, Imaz I, et al.: High-Resolution Human Kidney Molecular Histology by Imaging Mass Spectrometry of Lipids. *Analytical Chemistry* 2021, 93:9364–9372.
[70] Tian X, Xie B, Zou Z, Jiao Y, Lin L-E, Chen C-L, et al.: Multimodal Imaging of Amyloid Plaques: Fusion of the Single-Probe Mass Spectrometry Image and Fluorescence Microscopy Image. *Analytical Chemistry* 2019, 91:12882–12889.
[71] Rabe JH, Sammour DA, Schulz S, Munteanu B, Ott M, Ochs K, et al.: Fourier Transform Infrared Microscopy Enables Guidance of Automated Mass Spectrometry Imaging to Predefined Tissue Morphologies. *Scientific Reports* 2018, 8:313.
[72] Abdelmoula WM, Regan MS, Lopez BGC, Randall EC, Lawler S, Mladek AC, et al.: Automatic 3D Nonlinear Registration of Mass Spectrometry Imaging and Magnetic Resonance Imaging Data. *Analytical Chemistry* 2019, 91:6206–6216.
[73] Goodwin RJ, Mackay CL, Nilsson A, Harrison DJ, Farde L, Andren PE, et al.: Qualitative and Quantitative MALDI Imaging of the Positron Emission Tomography Ligands Raclopride (a D2 dopamine antagonist) and SCH 23390 (a D1 dopamine antagonist) in Rat Brain Tissue Sections Using a Solvent-free Dry Matrix Application Method. *Analytical Chemistry* 2011, 83:9694–9701.
[74] Huber K, Feuchtinger A, Borgmann DM, Li Z, Aichler M, Hauck SM, et al.: Novel Approach of MALDI Drug Imaging, Immunohistochemistry, and Digital Image Analysis for Drug Distribution Studies in Tissues. *Analytical Chemistry* 2014, 86:10568–10575.

©2022 The Authors. Creative Commons Attribution 4.0 International License

[75] Yuan Z, Zhou Q, Cai L, Pan L, Sun W, Qumu S, et al.: SEAM is a Spatial Single Nuclear Metabolomics Method for Dissecting Tissue Microenvironment. *Nature Methods* 2021, 18:1223–1232.

[76] Prideaux B, Dartois V, Staab D, Weiner DM, Goh A, Via LE, et al.: High-Sensitivity MALDI-MRM-MS Imaging of Moxifloxacin Distribution in Tuberculosis-infected Rabbit Lungs and Granulomatous Lesions. *Analytical Chemistry* 2011, 83:2112–2118.

[77] Zhang J, Du Q, Song X, Gao S, Pang X, Li Y, et al.: Evaluation of the Tumor-targeting Efficiency and Intratumor Heterogeneity of Anticancer Drugs Using Quantitative Mass Spectrometry Imaging. *Theranostics* 2020, 10:2621–2630.

[78] Treu A, Kokesch-Himmelreich J, Walter K, Holscher C, Rompp A: Integrating High-Resolution MALDI Imaging into the Development Pipeline of Anti-Tuberculosis Drugs. *Journal of the American Society for Mass Spectrometry* 2020, 31:2277–2286.

[79] Eberlin LS, Mulcahy JV, Tzabazis A, Zhang J, Liu H, Logan MM, et al.: Visualizing Dermal Permeation of Sodium Channel Modulators by Mass Spectrometric Imaging. *Journal of the American Chemical Society* 2014, 136:6401–6405.

[80] Bianga J, Bouslimani A, Bec N, Quenet F, Mounicou S, Szpunar J, et al.: Complementarity of MALDI and LA ICP Mass Spectrometry for Platinum Anticancer Imaging in Human Tumor. *Metallomics: Integrated Biometal Science* 2014, 6:1382–1386.

[81] Menetrey A, Legouffe R, Haouala A, Bonnel D, Rouits E, Bosq J, et al.: Tumor Distribution by Quantitative Mass Spectrometry Imaging of the Inhibitor of Apoptosis Protein Antagonist Xevinapant in Patients with Resectable Squamous Cell Carcinoma of the Head and Neck (EudraCT Number: 2014-004655-31). *Analytical Chemistry* 2022, 94:12333–12341.

[82] Randall EC, Emdal KB, Laramy JK, Kim M, Roos A, Calligaris D, et al.: Integrated Mapping of Pharmacokinetics and Pharmacodynamics in a Patient-derived Xenograft Model of Glioblastoma. *Nature Communications* 2018, 9:4904.

[83] He J, Luo Z, Huang L, He J, Chen Y, Rong X, et al.: Ambient Mass Spectrometry Imaging Metabolomics Method Provides Novel Insights into the Action Mechanism of Drug Candidates. *Analytical Chemistry* 2015, 87:5372–5379.

[84] Pang X, Gao S, Ga M, Zhang J, Luo Z, Chen Y, et al.: Mapping Metabolic Networks in the Brain by Ambient Mass Spectrometry Imaging and Metabolomics. *Analytical Chemistry* 2021, 93:6746—6754.

[85] Li X, Hang L, Wang T, Leng Y, Zhang H, Meng Y, et al.: Nanoscale Three-Dimensional Imaging of Drug Distributions in Single Cells via Laser Desorption Post-Ionization Mass Spectrometry. *Journal of the American Chemical Society* 2021, 143:21648–21656.

[86] Liu X, Hummon AB: Mass Spectrometry Imaging of Therapeutics from Animal Models to Three-dimensional Cell Cultures. *Analytical Chemistry* 2015, 87:9508–9519.

[87] Tobias F, McIntosh JC, LaBonia GJ, Boyce MW, Lockett MR, Hummon AB: Developing a Drug Screening Platform: MALDI-Mass Spectrometry Imaging of Paper-Based Cultures. *Analytical Chemistry* 2019, 91:15370–15376.

[88] Lukowski JK, Weaver EM, Hummon AB: Analyzing Liposomal Drug Delivery Systems in Three-Dimensional Cell Culture Models Using MALDI Imaging Mass Spectrometry. *Analytical Chemistry* 2017, 89:8453–8458.

[89] Cho CF, Wolfe JM, Fadzen CM, Calligaris D, Hornburg K, Antonio Chiocca E, et al.: Blood-Brain-Barrier Spheroids as an In Vitro Screening Platform for Brain-Penetrating Agents. *Nature Communications* 2017, 8:15623.

[90] RamalloGuevara C, Paulssen D, Popova AA, Hopf C, Levkin PA: Fast Nanoliter-Scale Cell Assays Using Droplet Microarray-Mass Spectrometry Imaging. *Advanced Biology* 2021, 5:e2000279.

[91] Moraleja I, Esteban-Fernandez D, Lazaro A, Humanes B, Neumann B, Tejedor A, et al.: Printing metal-spiked inks for LA-ICP-MS Bioimaging Internal Standardization: Comparison of the Different Nephrotoxic Behavior of Cisplatin, Carboplatin, and Oxaliplatin. *Analytical and Bioanalytical Chemistry* 2016, 408:2309–2318.

[92] Dexter A, Steven RT, Patel A, Dailey LA, Taylor AJ, Ball D, et al.: Imaging Drugs, Metabolites and Biomarkers in Rodent Lung: a DESI MS Strategy for the Evaluation of Drug-induced Lipidosis. *Analytical and Bioanalytical Chemistry* 2019, 411:8023–8032.

[93] Jiang H, Gao S, Hu G, He J, Jin H: Innovation in Drug Toxicology: Application of Mass Spectrometry Imaging Technology. *Toxicology* 2021, 464:153000.

[94] Zhao C, Xie P, Yong T, Wang H, Chung ACK, Cai Z: MALDI-MS Imaging Reveals Asymmetric Spatial Distribution of Lipid Metabolites from Bisphenol S-Induced Nephrotoxicity. *Analytical Chemistry* 2018, 90:3196–3204.

[95] Castellino S, Groseclose MR, Sigafoos J, Wagner D, de Serres M, Polli JW, et al.: Central Nervous System Disposition and Metabolism of Fosdevirine (GSK2248761), a Non-nucleoside Reverse Transcriptase Inhibitor: an LC-MS and Matrix-assisted Laser Desorption/Ionization Imaging MS Investigation into Central Nervous System Toxicity. *Chemical Research in Toxicology* 2013, 26:241–251.

[96] Asslan M, Lauzon N, Beus M, Maysinger D, Rousseau S: Mass Spectrometry Imaging in Zebrafish Larvae for Assessing Drug Safety and Metabolism. *Analytical and Bioanalytical Chemistry* 2021, 413:5135–5146.

[97] Yang J, Rendino L, Cassar S, Buck W, Sawicki J, Talaty N, et al.: Optimization of Zebrafish Larvae Sectioning for Mass Spectrometry Imaging. *Pharmaceuticals* 2022, 15:1230.

[98] Zhao X, Huang X, Zhang X, Shi J, Jia X, Zhu K, et al.: Distribution Visualization of the Chlorinated Disinfection Byproduct of Diazepam in Zebrafish with Desorption Electrospray Ionization Mass Spectrometry Imaging. *Talanta* 2022, 237:122919.

[99] Li H, Wei W, Xu H: Drug Discovery is An Eternal Challenge for the Biomedical Sciences. *Acta Materia Medica* 2022. DOI: 10.15212/AMM-2022-1001.

[100] Chen D, Du M, Huang Y, Xu Y, Chen Y, Ma L, et al.: Plasmonic Polydopamine-modified TiO2 Nanotube Substrates for Surface-assisted Laser Desorption/Ionization Mass Spectrometry Imaging. *Nano Research* 2022.

[101] Huang L, Nie L, Dai Z, Dong J, Jia X, Yang X, et al.: The Application of Mass Spectrometry Imaging in Traditional Chinese Medicine: A Review. *Chinese Medicine* 2022, 17:35.

[102] Gao L, Zhang Z, Wu W, Deng Y, Zhi H, Long H, et al.: Quantitative Imaging of Natural Products in Fine Brain Regions using Desorption Electrospray Ionization Mass Spectrometry Imaging (DESI-MSI): Uncaria Alkaloids as a Case Study. *Analytical and Bioanalytical Chemistry* 2022, 414:4999–5007.

©2022 The Authors. Creative Commons Attribution 4.0 International License

[103] Sun C, Ma S, Li L, Wang D, Liu W, Liu F, et al.: Visualizing the Distributions and Spatiotemporal Changes of Metabolites in Panax Notoginseng by MALDI Mass Spectrometry Imaging. *Journal of Ginseng Research* 2021, 45:726–733.

[104] Eckelmann D, Kusari S, Spiteller M: Occurrence and Spatial Distribution of Maytansinoids in Putterlickia Pyracantha, an Unexplored Resource of Anticancer Compounds. *Fitoterapia* 2016, 113:175–181.

[105] Tong Q, Zhang C, Tu Y, Chen J, Li Q, Zeng Z, et al.: Biosynthesis-based Spatial Metabolome of Salvia Miltiorrhiza Bunge by Combining Metabolomics Approaches with Mass Spectrometry-Imaging. *Talanta* 2022, 238:123045.

[106] Van de Plas R, Yang J, Spraggins J, Caprioli RM: Image Fusion of Mass Spectrometry and Microscopy: A Multimodality Paradigm for Molecular Tissue Mapping. *Nature Methods* 2015, 12:366–372.

[107] Yan X, Zhao X, Zhou Z, McKay A, Brunet A, Zare RN: Cell-Type-Specific Metabolic Profiling Achieved by Combining Desorption Electrospray Ionization Mass Spectrometry Imaging and Immunofluorescence Staining. *Analytical Chemistry* 2020, 92:13281–13289.

[108] Hale OJ, Cooper HJ: Native Mass Spectrometry Imaging of Proteins and Protein Complexes by Nano-DESI. *Analytical Chemistry* 2021, 93:4619–4627.

[109] Hale OJ, Hughes JW, Sisley EK, Cooper HJ: Native Ambient Mass Spectrometry Enables Analysis of Intact Endogenous Protein Assemblies up to 145 kDa Directly from Tissue. *Analytical Chemistry* 2022, 94: 5608–5614.

[110] Kuett L, Catena R, Ozcan A, Plüss A, Cancer Grand Challenges IMAXT Consortium, Schraml P, et al.: Three-dimensional Imaging Mass Cytometry for Highly Multiplexed Molecular and Cellular Mapping of Tissues and the Tumor Microenvironment. *Nature Cancer* 2022, 3:122–133.

[111] Mello MG, Westerhausen MT, Singh P, Doble PA, Wanagat J, Bishop DP: Assessing the Reproducibility of Labelled Antibody Binding in Quantitative Multiplexed Immuno-mass Spectrometry Imaging. *Analytical and Bioanalytical Chemistry* 2021, 413:5509–5516.

[112] Schulz D, Zanotelli VRT, Fischer JR, Schapiro D, Engler S, Lun XK, et al.: Simultaneous Multiplexed Imaging of mRNA and Proteins with Subcellular Resolution in Breast Cancer Tissue Samples by Mass Cytometry. *Cell Systems* 2018, 6:25–36.e5.

[113] Schapiro D, Jackson HW, Raghuraman S, Fischer JR, Zanotelli VRT, Schulz D, et al.: histoCAT: Analysis of Cell Phenotypes and Interactions in Multiplex Image Cytometry Data. *Nature Methods* 2017, 14:873–876.

[114] Yang J, Chaurand P, Norris JL, Porter NA, Caprioli RM: Activity-based Probes Linked with Laser-Cleavable Mass Tags for Signal Amplification in Imaging Mass Spectrometry: Analysis of Serine Hydrolase Enzymes in Mammalian Tissue. *Analytical Chemistry* 2012, 84:3689–3695.

[115] Rosas-Román I, Ovando-Vázquez C, Moreno-Pedraza A, Guillén-Alonso H, Winkler R: Open LabBot and RmsiGUI: Community Development Kit for Sampling Automation and Ambient Imaging. *Microchemical Journal* 2020, 152:104343.

[116] Korber A, Keelor JD, Claes BSR, Heeren RMA, Anthony IGM: Fast Mass Microscopy: Mass Spectrometry Imaging of a Gigapixel Image in 34 Minutes. *Analytical Chemistry* 2022, 94:14652–14658.

[117] Palmer A, Phapale P, Chernyavsky I, Lavigne R, Fay D, Tarasov A, et al.: FDR-Controlled Metabolite Annotation for High-Resolution Imaging Mass Spectrometry. *Nature Methods* 2017, 14:57–60.

[118] Tortorella S, Tiberi P, Bowman AP, Claes BSR, Ščupáková K, Heeren RMA, et al.: LipostarMSI: Comprehensive, Vendor-Neutral Software for Visualization, Data Analysis, and Automated Molecular Identification in Mass Spectrometry Imaging. *Journal of the American Society for Mass Spectrometry* 2020, 31:155–163.

[119] Semente L, Baquer G, Garcia-Altares M, Correig-Blanchar X, Rafols P: rMSIannotation: A Peak Annotation Tool for Mass Spectrometry Imaging Based on the Analysis of Isotopic Intensity Ratios. *Analytica Chimica Acta* 2021, 1171:338669.

[120] van Geenen F, Claassen FW, Franssen MCR, Zuilhof H, Nielen MWF: Laser Ablation Electrospray Ionization Hydrogen/Deuterium Exchange Ambient Mass Spectrometry Imaging. *Journal of the American Society for Mass Spectrometry* 2020, 31:249–256.

[121] Song X, Li J, Mofidfar M, Zare RN: Distinguishing between Isobaric Ions Using Microdroplet Hydrogen-Deuterium Exchange Mass Spectrometry. *Metabolites* 2021, 11:728.

[122] Mellinger AL, Muddiman DC, Gamcsik MP: Highlighting Functional Mass Spectrometry Imaging Methods in Bioanalysis. *Journal of Proteome Research* 2022, 21:1800–1807.

[123] Song X, Zang Q, Zhang J, Gao S, Zheng K, Li Y, et al.: X-dimensional Mass Spectrometry Imaging Discovers Spatially Resolved Metabolic Response. 15 March 2022, PREPRINT (Version 1) available at Research Square [https://doiorg/1021203/rs3rs-1432835/v1]. 2022.

[124] Sun C, Li T, Song X, Huang L, Zang Q, Xu J, et al.: Spatially Resolved Metabolomics to Discover Tumor-associated Metabolic Alterations. *Proceedings of the National Academy of Sciences (USA)* 2019, 116:52–57.

[125] Wang Z, Yang R, Zhang Y, Hui X, Yan L, Zhang R, et al.: Ratiometric Mass Spectrometry Imaging for Stain-Free Delineation of Ischemic Tissue and Spatial Profiling of Ischemia-Related Molecular Signatures. *Frontiers in Chemistry* 2021, 9:807868.

[126] Hamilton BR, Marshall DL, Casewell NR, Harrison RA, Blanksby SJ, Undheim EAB: Mapping Enzyme Activity on Tissue by Functional Mass Spectrometry Imaging. *Angewandte Chemie (International Ed in English)* 2020, 59:3855–3858.

[127] Takeo E, Fukusaki E, Shimma S: Mass Spectrometric Enzyme Histochemistry Method Developed for Visualizing In Situ Cholinesterase Activity in Mus musculus and Drosophila melanogaster. *Analytical Chemistry* 2020, 92:12379–12386.

[128] Song X, Zang Q, Zare RN: Hydrogen-Deuterium Exchange Desorption Electrospray Ionization Mass Spectrometry Visualizes an Acidic Tumor Microenvironment. *Analytical Chemistry* 2021, 93:10411–10417.

[129] Rubel O, Greiner A, Cholia S, Louie K, Bethel EW, Northen TR, et al.: OpenMSI: a High-Performance Web-based Platform for Mass Spectrometry Imaging. *Analytical Chemistry* 2013, 85:10354–10361.

[130] Liu X, Weaver EM, Hummon AB: Evaluation of Therapeutics in Three-dimensional Cell Culture Systems

©2022 The Authors. Creative Commons Attribution 4.0 International License

by MALDI Imaging Mass Spectrometry. *Analytical Chemistry* 2013, 85:6295–6302.

[131] McCombie G, Staab D, Stoeckli M, Knochenmuss R: Spatial and Spectral Correlations in MALDI Mass Spectrometry Images by Clustering and Multivariate Analysis. *Analytical Chemistry* 2005, 77:6118–6124.

[132] Torok S, Vegvari A, Rezeli M, Fehniger TE, Tovari J, Paku S, et al.: Localization of Sunitinib, its Metabolites and its Target Receptors in Tumour-bearing Mice: A MALDI-MS Imaging Study. *British Journal of Pharmacology* 2015, 172:1148–1163.

[133] Chen D, Xu Y, Huang Y, Chen Y, Zhao Y, Yan B, et al.: Mapping Molecular Signatures in Plant Leaves, Flowers, and Fruits by a TiO_2 Nanotube-based Plasmonic Chip for Imprint Mass Spectrometry Imaging. *ACS Agricultural Science & Technology* 2022. https://doi.org/10.1021/acsagscitech.2c00254.

[134] Cornett DS, Reyzer ML, Chaurand P, Caprioli RM: MALDI Imaging Mass Spectrometry: Molecular Snapshots of Biochemical Systems. *Nature Methods* 2007, 4:828–833.

[135] Kompauer M, Heiles S, Spengler B: Atmospheric Pressure MALDI Mass Spectrometry Imaging of Tissues and Cells at 1.4-μm Lateral Resolution. *Nature Methods* 2017, 14:90–96.

[136] Sabine Becker J: Imaging of Metals in Biological Tissue by Laser Ablation Inductively Coupled Plasma Mass Spectrometry (LA-ICP-MS): State of the Art and Future Developments. *Journal of Mass Spectrometry* 2013, 48:255–268.

[137] Peter Nemes AV: Laser Ablation Electrospray Ionization for Atmospheric Pressure, In Vivo, and Imaging Mass Spectrometry. *Analytical Chemistry* 2007, 79:8098–8106.

[138] Yifan M, Xiaowei S, Richard NZ: Laser Ablation Electrospray Ionization Achieves 5 μm Resolution Using a Microlensed Fiber. *Analytical Chemistry* 2022, 28:10278–10282.

[139] Robichaud G, Barry JA, Garrard KP, Muddiman DC: Infrared Matrix-Assisted Laser Desorption Electrospray Ionization (IR-MALDESI) Imaging Source Coupled to a FT-ICR Mass Spectrometer. *Journal of the American Society for Mass Spectrometry* 2013, 24:92–100.

[140] Bokhart MT, Manni J, Garrard KP, Ekelof M, Nazari M, Muddiman DC: IR-MALDESI Mass Spectrometry Imaging at 50 Micron Spatial Resolution. *Journal of the American Society for Mass Spectrometry* 2017, 28:2099–2107.

[141] Wiseman JM, Ifa DR, Venter A, Cooks RG: Ambient Molecular Imaging by Desorption Electrospray Ionization Mass Spectrometry. *Nature Protocols* 2008, 3:517–524.

[142] Unsihuay D, Yin R, Sanchez DM, Yang M, Li Y, Sun X, et al.: High-Resolution Imaging and Identification of Biomolecules using Nano-DESI Coupled to Ion Mobility Spectrometry. *Analytica Chimica Acta* 2021, 1186:339085.

[143] Swales JG, Strittmatter N, Tucker JW, Clench MR, Webborn PJH, Goodwin RJA: Spatial Quantitation of Drugs in Tissues using Liquid Extraction Surface Analysis Mass Spectrometry Imaging. *Scientific Reports* 2016, 6:37648.

[144] Swales JG, Tucker JW, Spreadborough MJ, Iverson SL, Clench MR, Webborn PJ, et al.: Mapping Drug Distribution in Brain Tissue using Liquid Extraction Surface Analysis Mass Spectrometry Imaging. *Analytical Chemistry* 2015, 87:10146–10152.

[145] Bich C, Touboul D, Brunelle A: Study of Experimental Variability in TOF-SIMS Mass Spectrometry Imaging of Biological Samples. *International Journal of Mass Spectrometry* 2013, 337:43–49.

[146] Legin AA, Schintlmeister A, Jakupec MA, Galanski MS, Lichtscheidl I, Wagner M, et al.: NanoSIMS Combined with Fluorescence Microscopy as a Tool for Subcellular Imaging of Isotopically Labeled Platinum-based Anticancer Drugs. *Chemical Science* 2014, 5:3135.

[147] Cordes J, Enzlein T, Marsching C, Hinze M, Engelhardt S, Hopf C, et al.: M2aia-Interactive, Fast, and Memory-Efficient Analysis of 2D and 3D Multi-modal Mass Spectrometry Imaging Data. *GigaScience* 2021, 10:giab049.

[148] Robichaud G, Garrard KP, Barry JA, Muddiman DC: MSiReader: An Open-source Interface to View and Analyze High Resolving Power MS Imaging Files on Matlab Platform. *Journal of the American Society for Mass Spectrometry* 2013, 24:718–721.

[149] Bokhart MT, Nazari M, Garrard KP, Muddiman DC: MSiReader v1.0: Evolving Open-source Mass Spectrometry Imaging Software for Targeted and Untargeted Analyses. *Journal of the American Society for Mass Spectrometry* 2018, 29:8–16.

[150] Stoeckli M, Staab D, Staufenbiel M, Wiederhold K-H, Signor L: Molecular Imaging of Amyloid β Peptides in Mouse Brain Sections using Mass Spectrometry. *Analytical Biochemistry* 2002, 311:33–39.

[151] Parry RM, Galhena AS, Gamage CM, Bennett RV, Wang MD, Fernandez FM: omniSpect: an Open MATLAB-based Tool for Visualization and Analysis of Matrix-assisted Laser Desorption/Ionization and Desorption Electrospray Ionization Mass Spectrometry Images. *Journal of the American Society for Mass Spectrometry* 2013, 24:646–649.

[152] Paschke C, Leisner A, Hester A, Maass K, Guenther S, Bouschen W, et al.: Mirion--A Software Package for Automatic Processing of Mass Spectrometric Images. *Journal of the American Society for Mass Spectrometry* 2013, 24:1296–1306.

[153] Kallback P, Nilsson A, Shariatgorji M, Andren PE: msIQuant--Quantitation Software for Mass Spectrometry Imaging Enabling Fast Access, Visualization, and Analysis of Large Data Sets. *Analytical Chemistry* 2016, 88:4346–4353.

[154] Bemis KD, Harry A, Eberlin LS, Ferreira C, van de Ven SM, Mallick P, et al.: Cardinal: An R Package for Statistical Analysis of Mass Spectrometry-Based Imaging Experiments. *Bioinformatics* 2015, 31:2418–2420.

[155] Lockwood TE, Westerhausen MT, Doble PA: Pew(2): Open-Source Imaging Software for Laser Ablation-Inductively Coupled Plasma-Mass Spectrometry. *Analytical Chemistry* 2021, 93:10418–10423.

[156] Kamila Chughtai RMAH: Mass Spectrometric Imaging for Biomedical Tissue Analysis. *Chemical Reviews* 2010, 110:3237–3277.

[157] Jardin-Mathe O, Bonnel D, Franck J, Wisztorski M, Macagno E, Fournier I, et al.: MITICS (MALDI Imaging Team Imaging Computing System): A New Open Source Mass Spectrometry Imaging Software. *Journal of Proteomics* 2008, 71:332–345.

[158] Race AM, Palmer AD, Dexter A, Steven RT, Styles IB, Bunch J: SpectralAnalysis: Software for the Masses. *Analytical Chemistry* 2016, 88:9451–9458.

[159] Shankar V, Tibshirani R, Zare RN. MassExplorer: A Computational Tool for Analyzing Desorption

©2022 The Authors. Creative Commons Attribution 4.0 International License

Electrospray Ionization Mass Spectrometry Data. *Bioinformatics*. 2021, 37:3688–3690.

[160] He J, Huang L, Tian R, Li T, Sun C, Song X, et al.: MassImager: A Software for Interactive and In-depth Analysis of Mass Spectrometry Imaging Data. *Analytica Chimica Acta* 2018, 1015:50–57.

[161] Huang L, Mao X, Sun C, Luo Z, Song X, Li X, et al.: A Graphical Data Processing Pipeline for Mass Spectrometry Imaging-based Spatially Resolved Metabolomics on Tumor Heterogeneity. *Analytica Chimica Acta* 2019, 1077:183–190.

[162] Schuerenberg M, Luebbert C, Deininger SO, Ketterlinus R, Suckau D: MALDI Tissue Imaging: Mass Spectrometric Localization of Biomarkers in Tissue Slices. *Nature Methods*. 2007, 4:462–462.

[163] Trede D, Schiffler SS, Becker M, Wirtz S, Strehlow J, Kobarg JH, et al.: O5. scils lab: Software for Analysis and Interpretation of large MALDIIMS Datasets. *OurCon* 2012:50.

[164] Hsieh Y, Chen J, Knemeyer I, Crossman L, Korfmacher WA: Visualization of First-Pass Drug Metabolism of Terfenadine by MALDI Imaging Mass Spectrometry. *Drug Metabolism Letters* 2008, 2:1–4.

[165] Tanaka Y, Hirata M, Shinonome S, Torii M, Nezasa KI, Tanaka H: Distribution Analysis of Epertinib in Brain Metastasis of HER2-Positive Breast Cancer by Imaging Mass Spectrometry and Prospect for Antitumor Activity. *Scientific Reports* 2018, 8:343.

[166] Morosi L, Spinelli P, Zucchetti M, Pretto F, Carrà A, D'Incalci M, et al.: Determination of Paclitaxel Distribution in Solid Tumors by Nano-Particle Assisted Laser Desorption Ionization Mass Spectrometry Imaging. *PloS One* 2013, 8:e72532.

[167] Katherine Margulis EAN, Beygui RE, Zare RN: Celecoxib Nanoparticles for Therapeutic Angiogenesis. *ASC Nano* 2015, 9:9416–9426.

[168] Kokesch-Himmelreich J, Treu A, Race AM, Walter K, Holscher C, Rompp A: Do Anti-tuberculosis Drugs Reach their Target? Horizontal Line High-Resolution Matrix-Assisted Laser Desorption/Ionization Mass Spectrometry Imaging Provides Information on Drug Penetration into Necrotic Granulomas. *Analytical Chemistry* 2022, 94:5483–5492.

[169] Bartelink IH, Prideaux B, Krings G, Wilmes L, Lee PRE, Bo P, et al.: Heterogeneous Drug Penetrance of Veliparib and Carboplatin Measured in Triple Negative Breast Tumors. *Breast Cancer Research* 2017, 19:107.

[170] Nguyen HN, Tanaka M, Li B, Ueno T, Matsuda H, Matsui T: Novel In Situ Visualisation of Rat Intestinal Absorption of Polyphenols via Matrix-assisted Laser Desorption/Ionisation Mass Spectrometry Imaging. *Scientific Reports* 2019, 9:3166.

[171] Morosi L, Matteo C, Meroni M, Ceruti T, Nerini IF, Bello E, et al.: Quantitative Measurement of Pioglitazone in Neoplastic and Normal tissues by AP-MALDI Mass Spectrometry Imaging. *Talanta* 2022, 237:122918.

[172] Buck A, Halbritter S, Spath C, Feuchtinger A, Aichler M, Zitzelsberger H, et al.: Distribution and Quantification of Irinotecan and Its Active Metabolite SN-38 in Colon Cancer Murine Model Systems Using MALDI MSI. *Analytical and Bioanalytical Chemistry* 2015, 407:2107–2116.

[173] Bokhart MT, Rosen E, Thompson C, Sykes C, Kashuba AD, Muddiman DC: Quantitative Mass Spectrometry Imaging of Emtricitabine in Cervical Tissue Model using Infrared Matrix-assisted Laser Desorption Electrospray Ionization. *Analytical and Bioanalytical Chemistry* 2015, 407:2073–2084.

[174] Jirasko R, Holcapek M, Kunes M, Svatos A: Distribution Study of Atorvastatin and Its Metabolites in Rat Tissues Using Combined Information from UHPLC/MS and MALDI-Orbitrap-MS Imaging. *Analytical and Bioanalytical Chemistry* 2014, 406:4601–4610.

[175] Liu J, Gingras J, Ganley KP, Vismeh R, Teffera Y, Zhao Z: Whole-body Tissue Distribution Study of Drugs in Neonate Mice Using Desorption Electrospray Ionization Mass Spectrometry Imaging. *Rapid Communications in Mass Spectrometry* 2014, 28:185–190.

[176] Luo Z, He J, Chen Y, He J, Gong T, Tang F, et al.: Air Flow-Assisted Ionization Imaging Mass Spectrometry Method for Easy Whole-body Molecular Imaging under Ambient Conditions. *Analytical Chemistry* 2013, 85:2977–2982.

[177] Pislyagin EA, Dmitrenok PS, Gorpenchenko TY, Avilov SA, Silchenko AS, Aminin DL: Determination of Cucumarioside A(2)-2 in Mouse Spleen by Radiospectroscopy, MALDI-MS and MALDI-IMS. *European Journal of Pharmaceutical Sciences* 2013, 49:461–467.

[178] Vallianatou T, Strittmatter N, Nilsson A, Shariatgorji M, Hamm G, Pereira M, et al.: A Mass Spectrometry Imaging Approach for Investigating How Drug-Drug Interactions Influence Drug Blood-Brain Barrier Permeability. *NeuroImage* 2018, 172:808–816.

[179] Holm NB, Deryabina M, Knudsen CB, Janfelt C: Tissue Distribution and Metabolic Profiling of Cyclosporine (CsA) in Mouse and Rat Investigated by DESI and MALDI Mass Spectrometry Imaging (MSI) of Whole-body and Single Organ Cryo-sections. *Analytical and Bioanalytical Chemistry* 2022, 414:7167–7177.

[180] Akakpo JY, Jaeschke MW, Etemadi Y, Artigues A, Toerber S, Olivos H, et al. Desorption Electrospray Ionization Mass Spectrometry Imaging Allows Spatial Localization of Changes in Acetaminophen Metabolism in the Liver after Intervention with 4-Methylpyrazole. *Journal of the American Society for Mass Spectrometry* 2022, 33:2094–2107.

[181] Nilsson A, Forngren B, Bjurstrom S, Goodwin RJA, Basmaci E, Gustafsson I, et al.: In Situ Mass Spectrometry Imaging and Ex Vivo Characterization of Renal Crystalline Deposits Induced in Multiple Preclinical Drug Toxicology Studies. *PloS one* 2012, 7:e47353.

[182] Meng Y, Gao C, Lu Q, Ma S, Hang W: Single-Cell Mass Spectrometry Imaging of Multiple Drugs and Nanomaterials at Organelle Level. *ACS Nano* 2021, 15:13220–13229.

[183] Sun N, Fernandez IE, Wei M, Wu Y, Aichler M, Eickelberg O, et al.: Pharmacokinetic and Pharmacometabolomic Study of Pirfenidone in Normal Mouse Tissues using High Mass Resolution MALDI-FTICR-Mass Spectrometry Imaging. *Histochemistry and Cell Biology* 2016, 145:201–211.

©2022 The Authors. Creative Commons Attribution 4.0 International License